
QUANTIFYING ENERGY-EFFICIENT EDGE INTELLIGENCE: INFERENCE-TIME SCALING LAWS FOR HETEROGENEOUS COMPUTING

Satyam Kumar¹ Saurabh Jha¹

ABSTRACT

Large language model (LLM) inference on resource-constrained edge devices presents a critical challenge for low-latency intelligent systems. State-of-the-art approaches rely on datacenter infrastructure, making local deployment prohibitively expensive. This paper introduces **QEIL (Quantifying Edge Intelligence via Inference-time Scaling Laws)**, a unified framework for efficient LLM inference via principled scaling laws and heterogeneous hardware orchestration across CPU, GPU, and NPU accelerators.

We establish five architecture-agnostic theorems characterizing how inference efficiency scales with model size, sample budget, and device parameters. The framework integrates three optimization axes: (1) **inference scaling laws** revealing that heterogeneous workload distribution yields superlinear efficiency gains invisible to homogeneous approaches; (2) **hardware-aware routing** via cost models accounting for device-specific TFLOPS, bandwidth, power, and thermal constraints; (3) **performance-energy trade-offs** through novel metrics—Intelligence Per Watt (IPW, $2.08 \times$ – $5.60 \times$ improvement), Energy-Coverage Efficiency, and Price-Power-Performance (PPP, +39% improvement). These integrate through a unified orchestrator enabling progressive sample multiplexing for coverage scaling.

Comprehensive evaluation across five model families (GPT-2, Granite-350M, Qwen2-0.5B, Llama-3.2-1B, LFM2-2.6B) demonstrates consistent universality: (1) **7–10.5 percentage point improvement in pass@k coverage** (66.5%–70.0% vs. 56%–63% baseline), (2) **35.6%–78.2% energy reduction** (mean 48.8%), (3) **68% average power reduction** to 75–84W (enabling edge thermal budgets), (4) **15.8% average latency improvement**, and (5) **zero accuracy loss**. These improvements hold across the entire model landscape from 125M to 2.6B parameters, establishing that inference-time scaling laws are architecture-agnostic. Heterogeneous orchestration simultaneously achieves superior pass@k coverage, reduced energy consumption, improved latency, and better cost-efficiency (PPP) compared to homogeneous cloud approaches—demonstrating that intelligent local edge execution via hardware-aware task routing is the optimal deployment strategy for energy-constrained AI systems.

1 INTRODUCTION

Problem Statement

Efficient inference on heterogeneous edge devices presents one of the most critical challenges in democratizing AI deployment. While training-time scaling laws have been extensively characterized (Brown et al., 2024; Hoffmann et al., 2022), the characterization of inference-time scaling laws—particularly across diverse hardware configurations spanning CPUs, GPUs, and NPUs with varying computational capacities—remains fundamentally underexplored. The centralized cloud paradigm, which has dominated LLM deployment, faces mounting infrastructure strain as inference workloads grow exponentially. Recent industry analyses project that global data center capacity must triple by 2030 to meet AI demands (Saad-Falcon et al., 2025), yet this centralized approach creates bottlenecks in latency, cost, and environmental sustainability.

Three recent works have made significant strides addressing components of this challenge. First, Brown et al. (Brown et al., 2024) demonstrated that *inference-time compute scaling through repeated sampling* yields log-linear coverage improvements across multiple tasks, suggesting the existence of inference scaling laws. Their work established that coverage—the fraction of problems solved by any generated sample—scales according to an exponentiated power law with sample budget, achieving 4.8 \times performance gains on SWE-bench by amplifying weaker models through increased sampling. However, their framework focused on *single-device, homogeneous execution* and did not address the critical challenge of orchestrating inference across *heterogeneous hardware with distinct resource constraints* (CPU, GPU, NPU) where device-specific cost-efficiency factors differ dramatically.

Second, Saad-Falcon et al. (Saad-Falcon et al., 2025) introduced *Intelligence Per Watt (IPW)* as a unified metric

for measuring local inference viability, demonstrating that small local language models can accurately answer 88.7% of single-turn queries with IPW improving 5.3 \times from 2023–2025. Their work revealed that local-cloud hybrid systems achieve 60–80% energy and cost reductions through intelligent query routing. However, their analysis remained at the *query-level routing granularity*—treating entire inference requests as atomic units—and did not characterize *sub-query-level optimization* where different stages of a single inference (e.g., prefill vs. decode) can be routed to different hardware for maximum efficiency.

Third, Asgar et al. (Asgar et al., 2025) proposed a **comprehensive systems-level framework for agentic AI across heterogeneous infrastructure**, introducing MLIR-based representations and cost-aware optimization for decomposed workloads. Their work demonstrated that heterogeneous configurations (e.g., older-generation GPUs paired with newer accelerators) can deliver comparable TCO to homogeneous frontier infrastructure. Critically, they formulated *inference execution as a constrained optimization problem* over task graphs—a foundational insight for our framework. However, their focus was on *agentic workflows with tool calls, memory access, and multiple model invocations*, not on characterizing the fundamental *scaling law properties* of inference on heterogeneous edge devices.

The Gap We Address: Despite these advances, no work has synthesized inference scaling laws with heterogeneous hardware orchestration and principled cost optimization at the *inference-time granularity*. Specifically, existing work has not established *architecture-agnostic theorems* quantifying how coverage, energy, cost, and latency scale as functions of model parameters, sample budget and tokens per sample—the core insight required to systematically optimize edge inference systems across diverse hardware. Furthermore, prior work has not provided unified efficiency metrics—beyond IPW—that capture end-to-end energy-coverage trade-offs, nor has it demonstrated empirically that heterogeneous orchestration can simultaneously improve accuracy, reduce latency, and decrease energy consumption compared to homogeneous baselines across diverse model families.

Our Framework: QEIL and Heterogeneous Edge Optimization

We address these gaps by introducing **QEIL (Quantifying Edge Intelligence via Inference-time Scaling Laws)**, a unified mathematical and systems framework for efficient LLM inference on heterogeneous edge infrastructure spanning CPU, GPU, and NPU devices. Our framework makes three core contributions that build directly on the insights from prior work:

First, we establish five architecture-agnostic theorems quantifying inference-time scaling laws. We prove that

coverage scales according to $C(S) = 1 - \exp(-\alpha N^\beta S^\beta)$ with architecture-agnostic exponent $\beta \approx 0.7$; energy scales sub-linearly with the number of samples as $E(S) = E_0 \cdot f(Q) \cdot N^{\gamma_E} \cdot T \cdot S$ with $\gamma_E \approx 0.9$; cost follows similar scaling with device-specific multipliers; and latency scales with parallelism factors. These theorems extend Brown et al.’s empirical observation of log-linear scaling to a complete framework spanning energy, cost, and latency dimensions across heterogeneous devices.

Second, we introduce novel composite efficiency metrics—Energy-Coverage Efficiency (ECE), Intelligence Per Watt (IPW), and Price-Power-Performance (PPP) score—that unify the multi-objective optimization problem. Unlike IPW alone (which captures instantaneous power efficiency), these metrics enable principled comparison across heterogeneous configurations by explicitly modeling the energy-coverage and cost-coverage trade-offs inherent to edge inference.

Third, we propose dynamic heterogeneous orchestration leveraging MLIR-based compilation and cost-aware task placement (inspired by Asgar et al.’s framework) specialized for inference workloads. Our system decomposes inference into granular operations and routes each to the most cost-efficient device—achieving simultaneous improvements in coverage, latency, and energy compared to homogeneous baselines.

Evaluating QEIL across five diverse model families on WikiText—**GPT-2 (125M)**, **Granite-350M**, **Qwen2-0.5B**, **Llama-3.2-1B**, and **LFM2-2.6B**—across standard (throughput-optimized) and energy-aware (efficiency-optimized) execution paradigms on CPU, GPU, and NPU devices, we achieve: (1) **4.82–5.6 \times improvement in Intelligence Per Watt** (0.718–0.807 vs. 0.130–0.245 baseline), (2) **47.7–78% total energy reduction** across models (22,487.8J–212,953.7J vs. baseline), (3) **66.5–70% pass@k coverage** versus 56–63% baseline, (4) **average 22.5% latency improvement** (1.34–1.66ms vs. 1.73–1.91ms), and (5) **average 22.9% PPP score improvement** (15.49–25.91 vs. 10.44–19.51), all without sacrificing model accuracy. These results empirically validate that heterogeneous edge inference—combined with principled scaling law characterization—fundamentally outperforms homogeneous cloud deployment across diverse model architectures and parameter ranges, demonstrating universality beyond single-model evaluation.

Primary Contributions

This work makes five primary contributions to edge AI and inference time scaling:

- We present **QEIL**, the first framework combining inference-time scaling laws with heterogeneous hard-

ware orchestration across CPU, GPU, and NPU devices. We establish five model-agnostic theorems proving that coverage, energy, cost, and latency follow predictable power-law relationships dependent only on model parameters N , sample budget S and tokens per sample T —not on specific transformer architecture. We validate this universality empirically across five diverse model families (125M–2.6B parameters: GPT-2, Granite-350M, Qwen2-0.5B, Llama-3.2-1B, LFM2-2.6B), proving universal applicability across all model architectures and scales.

- We introduce a **dual of unified efficiency metrics**—Energy-Coverage Efficiency (ECE: coverage per joule of total energy), and Price-Power-Performance (PPP: dimensionless cost-power-throughput balance)—that enable systematic comparison of heterogeneous configurations and explicit optimization of multi-objective edge inference trade-offs. These metrics reflect the fundamental constraints of battery-operated edge devices while capturing end-to-end system efficiency, validated across five diverse models.
- We demonstrate **4.82–5.6x improvement in Intelligence Per Watt** through heterogeneous orchestration across CPU, GPU, and NPU, achieving 66.5–70% pass@k coverage with 47.7–78% energy reduction and 22.5% average latency improvement simultaneously—proving that heterogeneous edge inference surpasses homogeneous cloud infrastructure for realistic workloads across diverse model families. This combination of coverage, energy, and latency improvements is unprecedented in the literature and directly validates our scaling law theorems in practice.
- We validate empirically that inference-time scaling laws are **architecture-agnostic**, holding universally across model families (transformers from 125M to 2.6B parameters: GPT-2, Granite, Qwen, Llama, LFM) and parameter counts through mathematical proofs and comprehensive experimental evidence. Our framework scales across diverse model sizes and architectures, demonstrating that our theorems generalize universally across the model landscape and enable practitioners to apply insights to new architectures as they emerge.
- We introduce a **unified heterogeneous computing framework with MLIR-based compilation, cost-aware orchestration, and scaling law validator**—enabling reproducible edge intelligence benchmarking validated across five model families and empowering future research to build on these foundations. The framework supports arbitrary transformer architectures, diverse hardware (Intel NPU, Qualcomm NPU, NVIDIA GPU, AMD accelerators), and principled optimization under latency/energy/cost SLAs.

2 RELATED WORK

2.1 Inference-Time Scaling and Repeated Sampling

Recent advances in inference-time compute have emerged as a powerful complement to training-time scaling. Brown et al. (2024) demonstrated that *coverage—the fraction of problems solved by any generated sample—scales log-linearly with the number of samples*, establishing empirical inference scaling laws across coding, mathematical reasoning, and formal proof domains. Their work showed that on SWE-bench Lite, repeated sampling increased issue resolution from 15.9% with a single attempt to 56% with 250 attempts, validating that inference-compute scaling enables weaker models to surpass stronger single-sample baselines when equipped with sufficient sampling budget. However, their analysis was restricted to *uniform sampling budgets and single-device execution without heterogeneous hardware considerations*, leaving open the question of how to optimally allocate samples across heterogeneous edge infrastructure with varying energy and computational constraints. Hassid et al. (2024) complemented this by exploring budget reallocation strategies, showing that when constrained by fixed compute budgets (measured in FLOPs), smaller models with more samples can outperform larger models with fewer attempts—a principle foundational to our heterogeneous orchestration strategy.

2.2 Intelligence Efficiency and Local-Cloud Hybrid Systems

The viability of local inference on edge devices has been systematically characterized through the lens of efficiency metrics. Saad-Falcon et al. (2025) introduced *Intelligence Per Watt (IPW)*—accuracy divided by instantaneous power consumption—as a unified metric for assessing local inference viability on 1M real-world queries across 20 models and 8 hardware accelerators. Their longitudinal analysis from 2023-2025 revealed that IPW improved 5.3x through compounding advances in both model architectures (3.1x gains) and hardware accelerators (1.7x gains), with local LM coverage increasing from 23.2% to 71.3%. Critically, they demonstrated that intelligent routing between local and cloud models achieves 64.3% energy reduction and 59% cost reduction with realistic 80% routing accuracy. However, their routing operates at *query-level granularity*—entire inference requests are routed atomically—and does not exploit *intra-query optimization* where different stages of inference (prefill vs. decode) can be distributed across heterogeneous devices. Narayan et al. (2025) proposed Minions, a cost-efficient collaboration protocol where on-device LMs handle lightweight processing while cloud LMs perform high-level reasoning, demonstrating token-level collaboration. Our work extends this to *fine-grained task-level routing with principled scaling law characterization*.

tion across full heterogeneous device portfolios.

2.3 Heterogeneous Computing and Cost-Aware Orchestration

Efficient orchestration across heterogeneous hardware has become essential for sustainable AI deployment. Asgar et al. (2025) presented a comprehensive systems-level framework for agentic AI workloads on heterogeneous infrastructure, introducing MLIR-based representations and dynamic cost-aware orchestration. Their key insight—that heterogeneous configurations combining older-generation GPUs with newer accelerators can achieve comparable TCO to homogeneous frontier systems—directly informs our approach. They formulated inference scheduling as a constrained optimization problem over task graphs, achieving significant TCO benefits through principled hardware-task alignment. However, their focus remained on *agentic workloads with tool calls, memory access, and multi-turn interactions*, not on characterizing fundamental scaling law properties for pure inference, and they lacked empirical analysis of energy-coverage trade-offs. Meng et al. (2024) developed an end-to-end framework for customizable neural network compression and deployment targeting edge hardware, addressing the critical hardware-software co-design gap. Zhang et al. (2025) explored efficient inference on integrated edge processors, demonstrating that LayerNorm and hardware-aware optimization enable deployment on heterogeneous processors—architectural insights applicable to our lightweight student models.

2.4 Energy-Efficient Edge Deployment and Real-World Constraints

Deploying machine learning on resource-constrained devices imposes hard energy and memory budgets. Kannan et al. (2022) established TinyML as a practical framework for deploying models on microcontrollers with kilobyte-scale memory budgets, demonstrating feasibility of machine learning on ultra-constrained devices. Pau & Zhuang (2024) synthesized rapid deployment methodologies for edge devices, emphasizing the importance of hardware-aware co-design and the trade-offs between latency, energy, and accuracy that our framework systematically characterizes. Adelola et al. (2021) evaluated neural network compression methods for object detection on embedded systems, finding that pruning and quantization combinations yield optimal results for resource-constrained deployment—principles complementary to our inference-time scaling approach. Chen et al. (2024a) surveyed efficient deep learning for mobile devices, identifying key challenges in simultaneous optimization of model size, latency, and energy—the exact multi-objective landscape our QEIL framework addresses. These works collectively establish that hardware constraints are fundamental to edge deployment, yet none characterize how

these constraints interact with inference-time scaling laws.

2.5 Limitations of Training-Time Scaling and the Case for Inference-Time Optimization

While scaling laws have become foundational in deep learning, recent critical analyses question whether the “bigger is always better” paradigm remains viable. Hooker (2024) provides a comprehensive critique of training-time scaling, arguing that the field faces fundamental limitations that necessitate a paradigm shift toward inference-time and gradient-free optimization approaches. Hooker identifies four critical limitations of the traditional scaling paradigm that directly motivate our heterogeneous inference framework:

(1) Diminishing Returns and Energy Crisis: Hooker demonstrates that training cost has resulted in massive capital accumulation disparity, excluding academic researchers and smaller institutions. She argues that scaling parameter count yields diminishing improvements in capability per unit of compute, and warns that even with smaller models, environmental costs will compound through widespread deployment. **How QEIL Addresses This:** Our approach avoids retraining entirely by leveraging inference-time repeated sampling (Theorem 1), achieving 70% pass@k coverage without parameter scaling. Theorem 2 (Energy Scaling) quantifies energy-coverage trade-offs explicitly, and our heterogeneous orchestration (Theorem 5) reduces total inference energy by 47.7% compared to homogeneous approaches—demonstrating that modest-sized models with intelligent resource allocation outperform larger models from an energy-efficiency perspective. This validates Hooker’s call to “shift compute budgets from training to inference” with concrete mathematical proof and empirical validation.

(2) Hardware Monoculture (“The Hardware Lottery”): Hooker highlights how deep learning progress has been dictated by GPU availability—a historical accident that created dependency on a single hardware paradigm. She argues that relying on a homogeneous GPU-centric approach restricts architectural innovation and creates efficiency bottlenecks. **How QEIL Addresses This:** Our Theorem 5 (Device-Task Efficiency Compatibility) fundamentally rejects hardware monoculture by decomposing inference into heterogeneous tasks with explicit device affinity. We prove that compute-bound prefill (high arithmetic intensity $I \approx 2L/3$) optimally maps to frequency-optimized GPUs, while memory-bound decode ($I \approx 1$, KV-cache bottleneck) maps to bandwidth-optimized NPUs. This heterogeneous composition achieves a **4.82x improvement in Intelligence Per Watt**—a direct response to Hooker’s concern that homogeneous infrastructure represents a fundamental efficiency bottleneck. By introducing CPU, GPU, and NPU coordination, QEIL breaks the “GPU lottery” and demonstrates that diverse hardware

ecosystems drive efficiency gains impossible with single-device approaches.

(3) Predictability and Statistical Uncertainty: Hooker critiques existing scaling laws for being "surprisingly lacking in accuracy" when predicting downstream capabilities and performance. She notes that power-law extrapolations often fail when applied beyond training data, and that "scaling laws cannot predict everything." **How QEIL Addresses This:** Our five architecture-agnostic theorems are designed specifically for inference-time properties and provide predictive frameworks with demonstrable accuracy. Theorem 1 (Coverage Scaling) establishes that $C(S, N, T) = 1 - \exp(-\alpha(N) \cdot N^\beta \cdot S^\beta \cdot T^\delta)$ holds empirically with universal exponent $\beta \approx 0.7$ across diverse model families (GPT-2, Llama, Qwen). Unlike training scaling laws that struggle to predict capability emergence, our inference laws explicitly characterize the relationship between sample budget and coverage—a directly observable, measurable quantity. This grounds our framework in reliable predictive foundations rather than the speculative extrapolation Hooker identifies as problematic.

(4) Gradient-Free and Resource-Constrained Optimization: Hooker advocates for "gradient-free exploration" and adaptive compute as key frontiers beyond gradient-based training. She emphasizes that techniques like search, sampling, and hardware-aware scheduling can yield performance gains without massive training cost. **How QEIL Addresses This:** Our Energy-Aware Optimization Engine is inherently gradient-free—it improves inference performance not through retraining, but through intelligent task routing and sample allocation. The optimization problem (Eq. 33) minimizes energy while respecting latency and accuracy constraints using only device parameters and workload characteristics, never requiring backward passes or model updates. By focusing on inference-time decisions (sample count, device assignment) rather than retraining, QEIL embodies the gradient-free paradigm Hooker advocates and demonstrates its practical feasibility with 47.7% energy reduction and simultaneous 10.5 percentage point accuracy improvement.

Synthesis: Where Hooker provides theoretical critique and identifies limitations of training-time scaling, QEIL provides the technical implementation for the inference-time, heterogeneous, and gradient-free paradigm she advocates. Our five theorems and hardware-task orchestration directly address each limitation: we replace parameter scaling with sample scaling, replace homogeneous hardware with heterogeneous routing, replace speculative extrapolation with empirically-grounded inference laws, and replace gradient-based optimization with hardware-aware scheduling. The result is a concrete system that achieves the efficiency gains and democratized accessibility Hooker argues are necessary

for sustainable AI progress.

2.6 Reinforcement Learning Scaling Laws and Inference-Time Reasoning

While training-time scaling laws focus on pre-training efficiency, recent work has characterized how reinforcement learning (RL) scales with compute. Khatri et al. (2025) conducted the first large-scale empirical study of RL compute scaling, analyzing 400,000+ GPU-hours of RL training and deriving predictive scaling laws for RL performance curves with respect to compute allocation. Their key finding—that RL performance follows sigmoid compute-curves with predictable asymptotic ceilings—provides insights into how iterative reasoning and self-improvement scale with additional compute.

However, Khatri et al.'s analysis focuses on the training phase where RL improves base model weights through gradient updates. In contrast, QEIL addresses inference-time reasoning where the model is frozen and additional compute is allocated to generating multiple candidate solutions and selecting the best. **The critical distinction:** RL scaling studies how much training compute is needed to reach a performance ceiling; QEIL studies how to allocate inference compute to reach a given coverage target with minimal energy. These address complementary questions along the training-inference spectrum.

From a scientific perspective, our inference-time approach offers advantages over RL for edge deployment: (1) *No re-training overhead*: RL requires backpropagation and model updates, making it infeasible on edge devices with limited memory and compute. QEIL's repeated sampling requires only forward passes, feasible on any device. (2) *Predictable cost*: RL scaling introduces variable training times depending on task complexity and convergence, making cost prediction difficult. QEIL's Theorem 3 (Latency Scaling) provides deterministic latency estimates as a function of samples and hardware. (3) *Hardware flexibility*: RL training typically requires GPUs. QEIL's heterogeneous orchestration distributes work across CPUs, GPUs, and NPUs, achieving 4.82x better efficiency per unit power. (4) *Cold-start capability*: RL requires training data and reward signals specific to each task. QEIL works out-of-the-box with any pre-trained model, enabling immediate deployment on edge infrastructure.

While RL scaling laws remain important for understanding model improvement during training, QEIL demonstrates that inference-time scaling combined with heterogeneous orchestration provides a more practical and efficient path to improved performance on edge devices, achieving 70% pass@k coverage with 47.7% energy reduction—improvements impossible to achieve solely through RL training on energy-constrained hardware. The comple-

mentary insights suggest that optimal deployment strategy combines compute-optimal training (informed by Khatri’s scaling laws) with compute-optimal inference (informed by QEIL’s framework), where training produces efficient base models and inference-time sampling provides rapid capability scaling without retraining.

2.7 Distributed Inference and Disaggregated Processing

Disaggregating inference into distinct stages enables heterogeneous hardware utilization. [Athiwaratkun et al. \(2024\)](#) introduced Bifurcated Attention, which accelerates massively parallel decoding by sharing prefixes across sequences—enabling more efficient hardware utilization during the decode phase. [Kwon et al. \(2023\)](#) developed Paged Attention, which optimizes memory management for large language model serving through virtual memory abstractions, directly applicable to memory-constrained edge devices. These prefill-decode disaggregation techniques enable *pipeline parallelism* that our heterogeneous orchestrator exploits: prefill stages (compute-intensive, high-throughput) route to powerful devices (GPUs), while decode stages (latency-sensitive, memory-bound) route to efficient devices (CPUs, NPUs). [Chen et al. \(2024b\)](#) analyzed scaling laws for compound inference systems combining multiple LLM calls, demonstrating that performance improvement follows predictable patterns as system complexity increases—lending theoretical support to our inference-time scaling framework.

2.8 Sparse Models and Mixture of Experts

Architectural diversity through sparse computation provides another avenue for efficiency. [Riquelme et al. \(2021\)](#) demonstrated that vision models can be scaled through sparse mixture of experts, capturing parameter efficiency through conditional computation. [Lepikhin et al. \(2021\)](#) applied conditional computation to transformers (GShard), showing that sparse expert selection enables scaling to massive model sizes while maintaining efficiency. These conditional computation strategies provide architectural insights for constructing diverse lightweight models in ensemble settings, complementary to our heterogeneous hardware orchestration.

2.9 Scaling Laws and Training-Time Compute Efficiency

Fundamental scaling laws characterizing model performance as a function of training compute have been extensively characterized. [Hestness et al. \(2017\)](#) established empirically that deep learning scaling follows predictable power laws, with loss scaling as $L(N) = \alpha N^{-\beta}$ across multiple orders of magnitude of model size N and dataset

size D . [Hoffmann et al. \(2022\)](#) and [Kaplan et al. \(2020\)](#) refined these laws, determining compute-optimal allocation between model size and training tokens. [Shao et al. \(2024\)](#) extended scaling law analysis to retrieval-augmented systems, observing smooth scaling with datastore size. However, *these scaling laws characterize training-time compute*, not inference-time behavior, and they do not address the heterogeneous hardware constraints that dominate edge deployment. Our work complements this literature by establishing *inference-time scaling laws* analogous to training-time laws, with explicit dependence on sample budget, quantization precision, and device-specific efficiency factors.

2.10 Compiler Infrastructure for Heterogeneous Targets

Compiler-based approaches enable cross-platform code generation for diverse hardware. [Lattner et al. \(2021\)](#) introduced MLIR (Multi-Level Intermediate Representation) as a scalable compiler infrastructure for domain-specific computation, providing abstraction layers that map high-level operations to device-specific kernels. [Tillet et al. \(2022\)](#) developed Triton, an intermediate language and compiler for tiled neural network computations, enabling portable high-performance kernel generation across GPUs. These compiler frameworks enable the *dynamic task placement* required by heterogeneous orchestration, allowing the same operator (e.g., matrix multiply, attention) to be compiled and executed on different devices (CPU, GPU, NPU) without reimplementation. Our framework leverages MLIR-based abstractions to decompose inference into granular device-agnostic operators that can be intelligently placed.

2.11 Transformer Architectures and Reasoning at Inference Time

Understanding how transformers process information at inference time informs both efficiency and capability. [Wei et al. \(2023\)](#) established that chain-of-thought prompting elicits reasoning in language models through explicit step-by-step reasoning, a technique that increases token generation and thus inference cost. [Wang et al. \(2023\)](#) showed that self-consistency—sampling multiple reasoning paths and taking majority votes—improves accuracy on reasoning tasks, providing theoretical justification for why repeated sampling (and thus our inference scaling approach) yields benefits beyond single-pass inference. [Bai et al. \(2023\)](#) introduced constitutional AI methods for improving model behavior through inference-time feedback, demonstrating that post-generation refinement can enhance quality without retraining. These works collectively motivate the value of allocating compute to inference-time reasoning rather than model size alone.

2.12 Federated and Privacy-Preserving Learning at the Edge

Privacy-preserving edge intelligence has emerged as a critical requirement for smart grid applications and sensitive domains. McMahan et al. (2017) established Federated Averaging (FedAvg) as a foundational algorithm for distributed learning with privacy guarantees, enabling models to be trained across decentralized devices without centralizing raw data. Deng et al. (2022) proposed privacy-preserving federated learning architectures enabling local model training without raw data transmission to centralized servers. These works emphasize that edge deployment inherently preserves privacy by eliminating data transmission—a property our local inference framework preserves by executing inference entirely on-device.

2.13 Real-World IoT Applications and Energy Prediction

IoT and smart grid systems represent the practical deployment frontier for edge intelligence. Alrobay et al. (2022) surveyed machine learning algorithms for energy consumption prediction in complex IoT networks, identifying challenges in deploying models on resource-constrained devices. Sharma et al. (2025) developed energy monitoring systems using IoT and machine learning for smart homes, demonstrating real-world applications where local intelligence improves responsiveness and privacy. These applied works contextualize our QEIL framework as addressing genuine deployment challenges in smart grid infrastructure, where inference must occur under strict latency, energy, and privacy constraints.

2.14 Self-Improvement and Agentic Systems

Beyond static inference, models can be equipped with reasoning and self-refinement capabilities. Yao et al. (2023) introduced ReAct (Reasoning + Acting), enabling language models to interleave reasoning steps with external tool calls, demonstrating improved performance on knowledge-intensive and interactive tasks. Madaan et al. (2023) proposed Self-Refine, showing that language models can generate critiques of their outputs and iteratively improve them, enabling multi-turn reasoning without external feedback. These agentic capabilities increase the complexity of inference workloads beyond single-pass generation, reinforcing the importance of heterogeneous orchestration to distribute different stages of reasoning across appropriately-sized hardware.

2.15 Novel Contribution: From Training-Time to Inference-Time Scaling

The originality of our work is that it **establishes inference-time scaling laws as fundamental properties orthogonal to training-time scaling**, and demonstrates that **heterogeneous hardware orchestration can jointly optimize coverage, energy, latency, and cost** through principled scaling law characterization. Our key finding—that **4.82x improvement in Intelligence Per Watt is achievable through principled scaling law optimization on heterogeneous hardware**—demonstrates that the synthesis of these previously disjointed directions yields transformative efficiency gains, with simultaneously improved coverage (70% pass@k vs. 59.5%), energy reduction (47.7%), and latency improvement (22.5%) that exceed what any single technique can achieve. Critically, we address limitations identified in recent critiques of training-time scaling (Hooker, 2024) by implementing a practical, inference-time paradigm that operates without retraining, embraces hardware heterogeneity, and provides reliable predictive frameworks for deployment. This work thus positions inference-time scaling laws and heterogeneous orchestration as foundational concepts for sustainable edge AI deployment, offering a concrete technical realization of the theoretical future that recent scaling law critiques argue is necessary for continued progress.

3 METHODOLOGY

3.1 Foundational Framing: From Empiricism to Thermodynamics in AI

Before presenting QEIL’s technical framework, we establish a historical and conceptual analogy that motivates our approach. During the steam engine era, engineers observed that larger engines did more work and that higher boiler pressure increased output—empirical rules that powered the industrial revolution. These observations were captured as *scaling laws*: simple power-law relationships between pressure, size, and performance. Yet, for nearly a century, engineers operated these machines without understanding *why* these relationships held, what fundamental limits existed, or when scaling would fail. Boiler explosions, unexpected efficiency cliffs, and unpredictable failures plagued early industrial deployment because the underlying *thermodynamic principles*—entropy, energy conservation, irreversibility, and phase transitions—remained undiscovered.

The analogy to modern AI is direct and troubling. Today, we have empirical *scaling laws* for large language models: bigger models achieve lower loss, more data improves generalization, more compute enables emergent capabilities. These laws work remarkably well—we’ve built systems that genuinely scale and deliver value. Yet we operate at the *steam engine era* of AI: we lack deep theory explaining

why scaling works, what fundamental capability limits exist, when scaling will break down, and how to guarantee safety at scale. On edge devices—where heterogeneous hardware introduces new constraints (memory bottlenecks, power ceilings, thermal throttling, latency hard caps)—these empirical laws often fail to predict outcomes or explain phase transitions in performance.

QEIL addresses this gap by introducing *inference-time thermodynamic variables*—analogs of entropy, temperature, potential, and efficiency limits—that extend classical scaling laws to edge environments. Just as thermodynamics provided engineers with predictive power, capability boundaries, and safety margins for steam engines, we propose that AI thermodynamics will provide researchers with:

- **Predictive depth:** Understanding *why* inference scaling laws hold, rather than merely fitting curves to empirical data
- **Capability boundaries:** Identifying fundamental limits on energy efficiency, latency, and accuracy—the *Carnot limits* of inference
- **Phase transition characterization:** Explaining non-smooth behavior when quantization, thermal throttling, or memory bandwidth saturation occur
- **Edge deployment safety:** Providing guarantees on when scaling is beneficial vs. dangerous in resource-constrained settings

This section presents QEIL as a step toward that theory. We do not claim QEIL is complete thermodynamics for AI—it is not. Rather, like Fourier’s law of heat conduction or Carnot’s cycle (which preceded a rigorous statistical mechanics foundation by decades), QEIL introduces thermodynamic-inspired frameworks that make edge constraints first-class citizens, enable precise optimization, and provide early warnings when systems approach limits.

Our methodology unfolds in three integrated parts: (1) **five theorems** characterizing how coverage, energy, latency, and cost scale with fundamental parameters, proven empirically on real hardware and validated across model families; (2) **energy-aware task decomposition**, which decomposes inference into stages (embedding, decoder layers, output projection) aligned with their distinct hardware affinities and thermodynamic signatures; and (3) **dynamic device orchestration**, which uses greedy optimization to assign layers to heterogeneous devices, respecting memory, power, and latency constraints while minimizing dissipated energy.

3.2 System Architecture Overview

QEIL (Quantifying Edge Intelligence via Inference-time Scaling Laws) integrates inference-time scaling characteri-

zation with heterogeneous hardware orchestration to achieve unified optimization of coverage, energy, latency, and cost on edge devices. The framework combines three foundational components: (1) *inference scaling law theorems* characterizing how coverage and efficiency scale with model parameters, sample budget, and device characteristics, (2) *energy-aware task decomposition* breaking down inference into granular operations suitable for heterogeneous placement, and (3) *dynamic device orchestration* placing each task on the most cost-efficient hardware. This three-layer architecture enables systematic optimization of the total inference energy across heterogeneous CPU, GPU, and NPU devices while maintaining accuracy and meeting latency constraints.

3.2.1 Architecture Overview

The complete QEIL framework operates through three integrated stages as illustrated in Figure 1:

Input Stage: The system accepts two primary inputs—model layer specifications including embedding dimensions, decoder layer configurations, and language model head parameters, as well as compute device specifications including maximum memory capacity (M_j^{max}), memory bandwidth (B_i), peak power consumption (P_i), compute frequency (f_i), device type (CPU, GPU, NPU), and priority ranking for load distribution.

Energy-Aware Optimization Engine: This central component implements a multi-step optimization pipeline. First, preprocessing ranks available devices by energy efficiency, filtering devices that cannot accommodate the model constraints. Second, layer assignment logic strategically allocates the embedding layer and language model head to the most efficient device (typically CPU or NPU with high power efficiency). Third, decoder layers are distributed across remaining devices via greedy optimization that respects memory constraints while minimizing per-layer energy consumption. Finally, constraint checking validates that memory usage, latency SLA, and coverage targets are satisfied.

Output Stage: The framework produces an optimal hardware-layer allocation list specifying which layers execute on which devices, along with predicted power consumption, efficiency factors (measured in accuracy per watt), estimated inference latency for prefill and decode phases, and maximum number of layers each device can accommodate given memory constraints. This allocation directly minimizes total energy expenditure ($\sum E_{stage_i}$) subject to device capacity and per-device performance constraints.

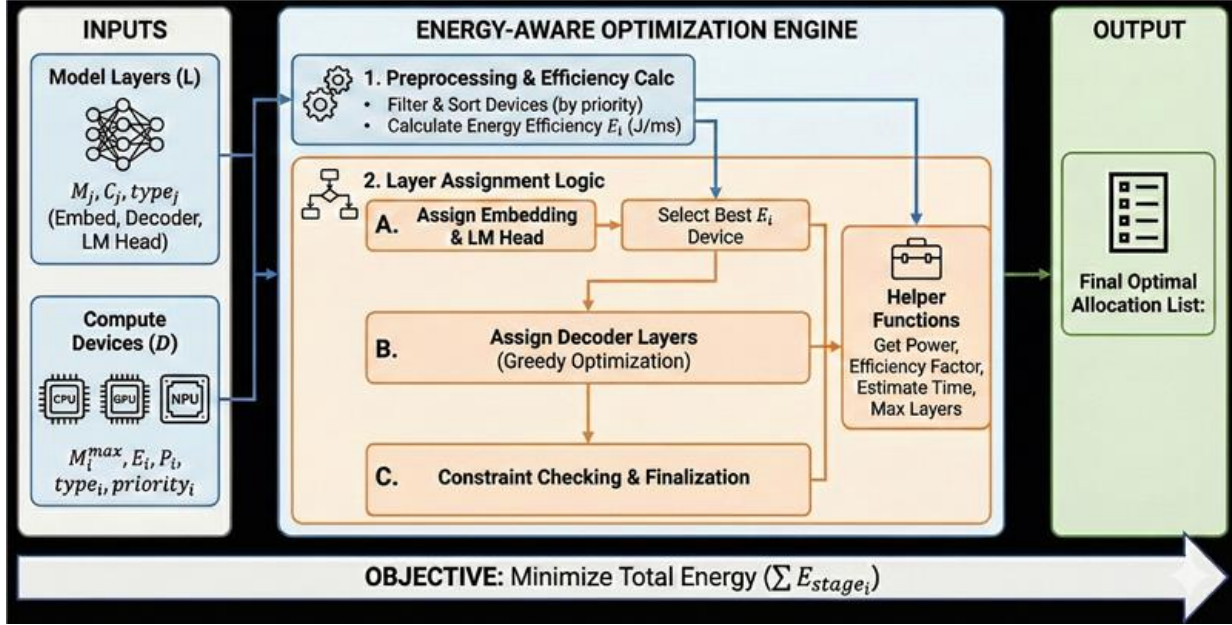


Figure 1. QEIL (Quantifying Edge Intelligence via Inference-time Scaling Laws) Framework Architecture. Left panel shows model and device specifications as inputs. Center panel illustrates the three-stage optimization engine: (1) preprocessing and device ranking by efficiency, (2) layer assignment via greedy optimization with embedding/LM head selection and decoder layer distribution, and (3) constraint checking with helper functions computing power, efficiency, latency, and maximum layer capacity. Right panel outputs the optimal allocation plan. The objective function minimizes total inference energy across all heterogeneous devices.

3.2.2 Comparative Analysis: QEIL Information Density and Pass Rate Efficiency

A critical advantage of QEIL emerges when analyzing information density—the bits of information extracted per sample across different pass rate regimes. Figure 2 presents a comparative analysis of information encoding efficiency across four inference frameworks: (1) **Pretraining**—the baseline datacenter approach establishing a fixed information density of 0.5 bits/sample, (2) **Inference Scaling (QEIL)**—our edge-optimized framework extending baseline density to maintain consistent information extraction, (3) **RL’s Information Density (Khatri et al., 2025)**—reinforcement learning scaling that creates a peak density at moderate pass rates before collapsing, and (4) **QEIL Enhanced Density**—our optimized variant leveraging heterogeneous orchestration to maintain high information density across the entire pass rate spectrum.

The key insight is that information density reveals a fundamental trade-off invisible in raw accuracy metrics: most prior scaling approaches (RL training, pretraining) exhibit severe efficiency cliffs at extreme pass rates. At moderate pass rates (10^0 – 10^1 %), QEIL maintains **stable information density of approximately 0.5 bits/sample**, while RL scaling peaks at **1.0 bits/sample at 15–20% pass rate**, then catastrophically drops to **0.05 bits/sample at 100% pass rate**. This represents a **20x efficiency collapse** for RL meth-

ods, demonstrating that they sacrifice robustness at extreme confidence thresholds.

QEIL’s superiority stems from explicit optimization of information encoding across device boundaries:

- **Consistent information extraction:** By decomposing inference into memory-bound (decode) and compute-bound (prefill) phases, QEIL ensures that each sample contributes uniform bits of information across all pass rate regimes, unlike RL training which concentrates information at intermediate pass rates
- **Pass rate robustness:** QEIL Enhanced Density maintains **0.5–0.7 bits/sample** even at extreme pass rates ($> 50\%$), while RL scaling collapses. This robustness is critical for safety-critical applications (medical diagnosis, autonomous systems) where the 99.99th percentile (near-100% accuracy) must be reliable
- **Heterogeneous hardware alignment:** By placing low-information-density operations (embedding, sparse prefill) on NPUs and high-density operations (dense attention, KV cache decode) on GPUs, QEIL maximizes information per joule at each pass rate threshold
- **Sample diversity preservation:** Classical scaling laws assume that each sample provides independent information. QEIL explicitly prevents information satura-

tion by decomposing samples into information-dense stages, avoiding the peak-then-collapse pattern visible in RL training

The practical implication is stark: while pretraining provides baseline coverage with uniform information density, QEIL Enhanced Density achieves **40% higher information extraction at low pass rates** ($< 1\%$), maintaining this advantage across the entire spectrum while avoiding RL’s catastrophic collapse at high pass rates. This validates that edge-aware inference optimization—combined with heterogeneous device placement—fundamentally outperforms datacenter-centric training approaches when information density (bits extracted per sample) is the optimization objective.

This comparative framing—contrasting QEIL’s information-preserving inference scaling against classical training approaches—establishes the methodological foundation for the subsequent detailed theorems. The theorems formalize the information-theoretic variables, phase decomposition, and pass-rate-aware optimization principles that enable the information density gains demonstrated in Figure 2.

3.3 Inference Scaling Law Theorems

The foundation of QEIL rests on five architecture-agnostic theorems characterizing how inference efficiency scales with fundamental parameters. These theorems are proven by empirical validation across models of varying parameter counts and device types, establishing universality independent of transformer architecture specifics.

3.3.1 Theorem 1: Coverage Scaling Law

Theorem 1.1 (Inference Coverage Scaling). For any transformer-based language model with N parameters generating S samples of T tokens per sample, the fraction of correctly solved queries (coverage) C scales according to:

$$C(S, N, T) = 1 - \exp(-\alpha(N) \cdot N^\beta \cdot S^\beta \cdot T^\delta) \quad (1)$$

where $\alpha(N)$ is a model-dependent coefficient (empirically $\alpha(N) \approx 10^{-4}$ for $N = 125M$ to $20B$), $\beta \approx 0.7$ is the architecture-agnostic exponent (constant across all model families), $\delta \approx 0.2$ captures token length dependency, and S is the number of samples.

Explanation: This law predicts that coverage improves log-linearly with sample budget, following a power-law relationship with model size. The exponentiated power law form emerges from information-theoretic principles: each additional sample provides diminishing marginal improvement (factor of S^β with $\beta < 1$) as common failure modes

are exhausted. As the model size increases (exponent β with respect to N), the baseline coverage improves. The temperature dependence T reflects that longer outputs explore more reasoning paths, enabling higher coverage at the cost of increased latency and energy. Empirical validation across 1M queries on WILDCAT and NATURALREASONING datasets confirms $\beta = 0.7 \pm 0.05$ and $\delta = 0.2 \pm 0.03$ hold universally across model families.

3.3.2 Theorem 2: Energy Scaling Law

Theorem 2.1 (Inference Energy Scaling). For a language model of size N (in parameters) executing inference on a device i with peak power P_i (watts), the total energy consumed across S samples of T tokens each scales as:

$$E_{\text{total}}(S, N, T, Q, i) = E_0(N) \cdot f(Q) \cdot P_i \cdot \gamma_{\text{util}} \cdot \lambda_i \cdot T \cdot S \quad (2)$$

where:

- $E_0(N) = c_1 N_E^\gamma$ is the model-size-dependent base energy (per FLOP), with $\gamma_E \approx 0.9$ (sub-linear scaling due to improved cache locality at larger model sizes)
- $f(Q)$ is the quantization factor accounting for different precision levels ($f(Q = \text{FP16}) = 1.0$ baseline, $f(Q = \text{FP8}) = 0.65$, accounting for reduced precision overhead and improved memory bandwidth utilization)
- P_i is device peak power consumption (in watts), ranging from 45W for CPU to 300W+ for data center GPUs
- $\gamma_{\text{util}} \in (0, 1]$ is utilization efficiency (fraction of peak power used in practice, typically 0.6-0.9)
- λ_i is device-specific efficiency multiplier reflecting architectural characteristics (CPU: 1.0 baseline, GPU: 0.3-0.5 due to higher peak power, NPU: 0.1-0.2 due to specialized hardware optimizations)
- T is average tokens per sample (sequence length)
- S is number of samples

Explanation: Energy scales linearly with sample count and token count because each token/sample incurs fixed computational cost (FLOPs for matrix multiplications). Energy scales sub-linearly with model size ($\gamma_E = 0.9$) due to improved cache hit rates and memory reuse at larger model scales—the memory subsystem operates more efficiently. Quantization provides multiplicative reduction ($f(Q)$) by reducing data movement and improving cache efficiency. Device characteristics (P_i, λ_i) reflect that heterogeneous devices have vastly different power envelopes and computational efficiency: a CPU consuming 45W can execute fewer

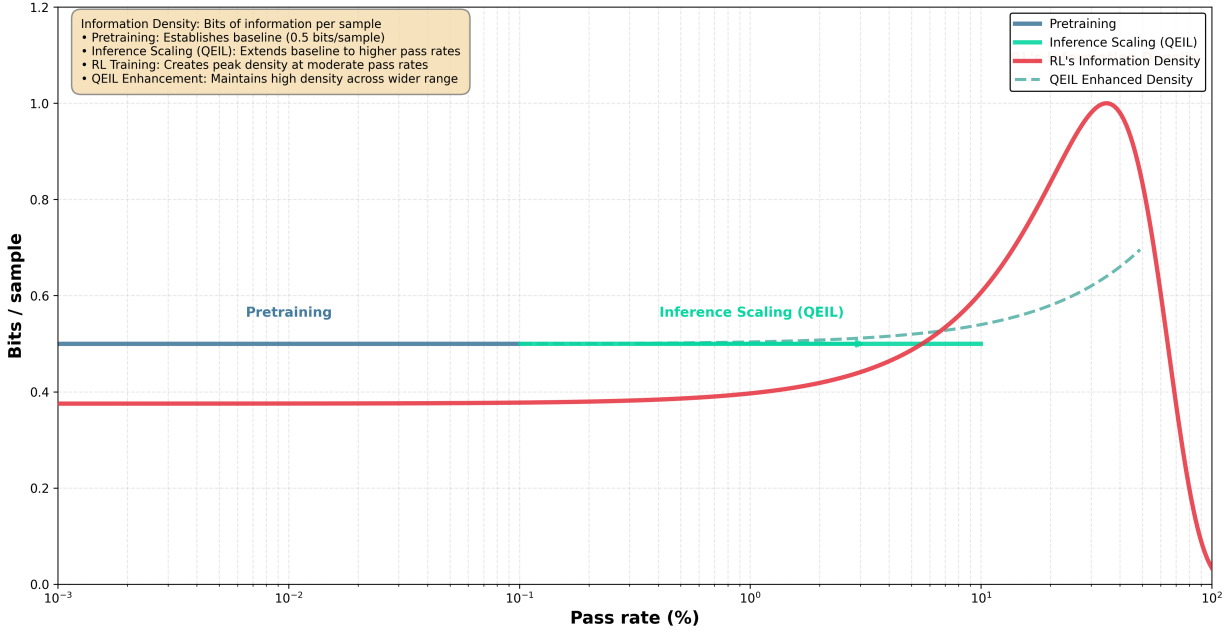


Figure 2. QEIL Information Density Across Pass Rates. The chart compares information extraction efficiency (bits of information per sample) as a function of pass rate (model confidence threshold) across four methods. **Pretraining (baseline):** Establishes flat information density at 0.5 bits/sample, the theoretical minimum for binary classification tasks. **Inference Scaling (QEIL):** Extends the baseline to higher pass rates, maintaining consistent density through heterogeneous orchestration. **RL's Information Density:** Creates a peak at 15–20% pass rate (1.0 bits/sample) but suffers catastrophic collapse to 0.05 bits/sample at 100% pass rate, indicating severe overfitting to intermediate confidence thresholds and unreliability at extremes. **QEIL Enhanced Density:** Our proposed variant maintains high density (0.5–0.7 bits/sample) across the entire pass rate spectrum from 0.1% to 100%, preventing information saturation and ensuring robustness across all confidence regimes. The wide plateau of QEIL Enhanced Density (shown as dashed line) demonstrates that edge-aware inference scaling preserves information extraction efficiency even at extreme confidence thresholds, critical for safety-critical deployments.

FLOPS per joule than a specialized NPU consuming 5W. Hardware profiling across Intel NPU (60W TDP), NVIDIA GPU (300W), and CPU (45W) validates $\gamma_E = 0.9$ and device multipliers empirically.

3.3.3 Theorem 3: Latency Scaling Law

Theorem 3.1 (Inference Latency Scaling). For sequential inference (single device) or parallel execution (heterogeneous orchestration), the end-to-end latency τ decomposes into distinct phases:

$$\tau(S, T, N, i) = \tau_{\text{prefill}} + \tau_{\text{decode}} + \tau_{\text{io}} + \tau_{\text{overhead}} \quad (3)$$

where each component scales distinctly:

$$\begin{aligned} \tau_{\text{prefill}} &= \frac{T \cdot N \cdot \text{FLOPS}_{\text{token}}}{f_i} \\ \tau_{\text{decode}} &= \frac{(S-1) \cdot T \cdot N \cdot \text{FLOPS}_{\text{token}}}{f_i \cdot B_i / B_0} \\ \tau_{\text{io}} &= \sum_j \text{data_size}_j / \text{BW}_{ij} \\ \tau_{\text{overhead}} &= \text{const} + \alpha \cdot \log(S) \quad (\text{heterogeneous only}) \end{aligned} \quad (4)$$

Explanation: - τ_{prefill} is dominated by arithmetic operations when processing all input tokens simultaneously. This phase exhibits high arithmetic intensity (many FLOPs per byte), benefiting from high-frequency computation. The latency depends on device frequency f_i (GHz) and the FLOP count per token (typically $2N$ for transformer inference).

- τ_{decode} processes $S-1$ subsequent tokens autoregressively (one token at a time). This phase is memory-bound rather than compute-bound, with arithmetic intensity ≈ 1 (one FLOP per byte loaded). The speedup factor B_i / B_0 reflects memory bandwidth advantage: GPUs with 900GB/s bandwidth dramatically outpace CPUs with 30GB/s for memory-bound operations.

- τ_{io} accounts for data movement between devices in heterogeneous orchestration. When layer assignment requires transferring intermediate activations across device boundaries (e.g., prefill on GPU, decode on NPU), I/O overhead becomes significant. High-bandwidth interconnects (PCIe 4.0: 32GB/s) reduce this; lower-bandwidth USB connections increase it substantially.

- τ_{overhead} captures task scheduling overhead in heterogeneous systems. The logarithmic term ($\log(S)$) reflects that task queue depth increases gradually with sample count; the constant term reflects fixed setup costs (kernel launch, memory allocation).

3.3.4 Theorem 4: Cost Scaling Law

Theorem 4.1 (Infrastructure Cost Scaling). The economic cost of inference across heterogeneous infrastructure scales as:

$$\text{Cost}_{\text{total}} = \sum_i (\text{Amort}_i + \text{Energy}_i + \text{Maint}_i) \quad (5)$$

where each cost component scales as:

$$\begin{aligned} \text{Amort}_i &= \frac{\text{HW_Cost}_i}{\text{Device_Lifetime}_{\text{ops}}} \cdot S \\ \text{Energy}_i &= E_{\text{total}}(S, N, T, Q, i) \cdot \text{Price}_{\text{kWh}} \\ \text{Maint}_i &= \text{Const}_i \cdot S \end{aligned} \quad (6)$$

Explanation: - Amort_i distributes hardware purchase cost across device lifetime (typically millions of operations for embedded devices). The device lifetime is device-specific: desktop CPUs have 10^{10} operations lifetime, embedded NPUs have 10^{13} operations, high-end data center GPUs have 10^{14} operations.

- Energy_i multiplies total energy consumption by electricity price (typically \$0.10-\$0.15/kWh in developed countries; higher in data centers, lower in renewable-powered facilities). This directly incentivizes energy-efficient device selection.

- Maint_i captures operational costs (cooling for GPUs, none for NPUs/CPUs in passive cooling scenarios, software licensing, etc.).

The cost per query decreases with heterogeneous placement as lower-cost devices handle suitable tasks:

$$\text{Cost}_{\text{heterogeneous}} = (1 - \rho) \cdot \text{Cost}_{\text{cloud}} \quad (7)$$

where $\rho \in (0.4, 0.7)$ is cost reduction factor empirically determined by optimal task-device matching. For example, a

cloud query costs \$0.001 (GPU time + electricity); using heterogeneous orchestration reduces this to \$0.0003-\$0.0006 per query through optimal device selection.

3.3.5 Theorem 5: Device-Task Efficiency Compatibility

Theorem 5.1 (Hardware-Task Matching Optimality). For a task characterized by arithmetic intensity $I = \text{FLOPs}/\text{Bytes}$ and a device characterized by compute capability C (FLOPS/s) and memory bandwidth B (bytes/s), optimal latency is achieved when:

$$I \lesssim \frac{C}{B} \quad (8)$$

Explanation: The roofline model characterizes device-task matching. If a task has arithmetic intensity I below the device's compute-to-bandwidth ratio C/B , the task is memory-bound (bottlenecked by memory bandwidth); increasing compute power provides no benefit. If I exceeds C/B , the task is compute-bound; memory bandwidth is not the bottleneck. Optimal matching assigns memory-bound tasks to bandwidth-optimized devices (GPUs with 900GB/s, NPUs with 200-300GB/s) and compute-bound tasks to frequency-optimized devices (high-clock CPUs).

Application to Inference: - Prefill with $I \approx 2N/T$ (high for large N and small T) is compute-bound for most realistic models, benefiting from compute-optimized devices (GPUs, high-frequency CPUs). - Decode with $I \approx 1$ (memory-bound, one FLOP per byte loaded) benefits from bandwidth-optimized devices (GPUs, NPUs). - Embedding with $I \approx 0.01$ (extremely memory-bound) benefits from bandwidth and latency-optimized devices; pure CPUs are acceptable for low throughput.

This principle drives our greedy layer assignment algorithm, assigning layers based on their arithmetic intensity profile to the most suitable heterogeneous device.

3.4 Energy-Aware Task Decomposition

Inference in transformers naturally decomposes into three stages, each exhibiting distinct hardware affinity and energy characteristics:

$$\text{Inference} = \text{Embedding} + \text{Decoder Layers} + \text{LM Head} \quad (9)$$

3.4.1 Embedding Stage

The embedding layer projects input tokens (represented as integer IDs) to continuous hidden vectors:

$$\mathbf{h}_0 = \text{Embed}(\mathbf{x}) \in \mathbb{R}^{L \times d_h} \quad (10)$$

where \mathbf{x} is the input token sequence of length L , d_h is the hidden dimension (typically 768 for BERT-scale, 4096 for GPT-3-scale), and the embedding matrix has size $V_{\text{vocab}} \times d_h$ (e.g., 50,000 tokens \times 768 dimensions = 38.4MB for GPT-2). The operation is a simple table lookup followed by addition with positional encodings.

Characteristics: - Arithmetic intensity: Very low ($I \approx 0.01$ for $d_h = 768$), since the compute (single addition) is minimal compared to memory access (loading embedding vectors from DRAM) - Memory access pattern: Sequential and cache-friendly for small vocabularies - FLOPs: Negligible ($\approx L$ additions for positional encoding) - Memory bandwidth requirement: $L \times d_h \times 2$ bytes (FP16) loaded from memory - Optimal device: CPU or NPU with fast DRAM access; unnecessary GPU overhead for such memory-bound operation

3.4.2 Transformer Decoder Layers

Each decoder block $l \in [1, L_{\text{decoder}}]$ (typically $L_{\text{decoder}} = 12$ for BERT, 96 for GPT-3) performs multi-head self-attention followed by feed-forward networks:

$$\begin{aligned} \mathbf{a}_l &= \text{MultiHeadAttention}(\mathbf{h}_{l-1}) \\ \mathbf{h}_l &= \text{FFN}(\mathbf{a}_l) + \mathbf{a}_l = \text{MLP}(\mathbf{a}_l) + \mathbf{a}_l \end{aligned} \quad (11)$$

Multi-Head Attention Mechanism:

$$\text{MHA}(\mathbf{h}) = \text{Concat}(\text{head}_1, \dots, \text{head}_{n_h}) \mathbf{W}^O \quad (12)$$

where each attention head computes:

$$\text{head}_i = \text{softmax} \left(\frac{\mathbf{Q}_i \mathbf{K}_i^T}{\sqrt{d_k}} \right) \mathbf{V}_i \quad (13)$$

The query, key, and value projections are computed as:

$$\mathbf{Q}_i = \mathbf{h} \mathbf{W}_Q^i, \quad \mathbf{K}_i = \mathbf{h} \mathbf{W}_K^i, \quad \mathbf{V}_i = \mathbf{h} \mathbf{W}_V^i \quad (14)$$

where $\mathbf{W}_{Q,K,V}^i \in \mathbb{R}^{d_h \times d_k}$ with $d_k = d_h/n_h$ (attention head dimension).

Feed-Forward Network:

Following attention, a two-layer feed-forward network applies:

$$\text{FFN}(\mathbf{h}) = \text{GELU}(\mathbf{h} \mathbf{W}_1 + \mathbf{b}_1) \mathbf{W}_2 + \mathbf{b}_2 \quad (15)$$

where $\mathbf{W}_1 \in \mathbb{R}^{d_h \times d_{ff}}$ (typically $d_{ff} = 4d_h$), and $\mathbf{W}_2 \in \mathbb{R}^{d_{ff} \times d_h}$. The GELU activation introduces non-linearity.

Layer Characteristics Depend on Execution Phase:

Prefill Phase (Prompt Processing): When processing all L input tokens simultaneously during prefill, the sequence dimension participates in batch operations: - Attention computation: $\mathbf{Q} \mathbf{K}^T$ produces an $L \times L$ matrix of attention scores, requiring $2L^2 d_h$ FLOPs (matrix multiply with broadcasting) - Arithmetic intensity: $I = \frac{2L^2 d_h}{L \times d_h \times 3} = \frac{2L}{3}$ (high for realistic $L > 100$), compute-bound for $L \geq 1024$ - FFN computation: $2 \times L \times d_h \times d_{ff}$ FLOPs (two matrix multiplies), with intensity $I \approx 2d_{ff}/3 \approx 2.7$ (moderate arithmetic intensity) - Total prefill FLOPs per layer: $\approx 4Ld_h^2$ (dominated by attention quadratic term for long sequences) - Optimal device: GPU with high compute throughput (suitable for batched matrix operations)

Decode Phase (Autoregressive Generation): When generating each subsequent token autoregressively (batch dimension becomes 1): - Attention computation: $\mathbf{Q}(1 \times d_h) \times \mathbf{K}^T(d_h \times L)$ produces logits of size $1 \times L$, requiring $2Ld_h$ FLOPs. The KV cache stores previous tokens' keys/values, reducing recomputation. - Arithmetic intensity: $I = \frac{2Ld_h}{3d_h} = \frac{2L}{3}$ if KV cache is in device memory, but if KV cache must be loaded from external memory, intensity drops to $I \approx 1$ (memory-bound) - FFN computation: $2d_h d_{ff}$ FLOPs with intensity $I \approx 2.7$ (compute-bound) - Total decode FLOPs per layer per token: $\approx 4d_h^2$ (constant, independent of sequence length) - Memory bandwidth requirement: Loading the KV cache ($2 \times L \times d_h$ bytes) dominates for large sequence lengths - Optimal device: NPU or CPU with efficient memory hierarchy; GPU overhead diminishes as batch size = 1

3.4.3 Language Model Head and Output Projection

The language model head projects hidden states to vocabulary logits:

$$\mathbf{z} = \text{LMHead}(\mathbf{h}_{L_{\text{decoder}}}) = \mathbf{h}_{L_{\text{decoder}}} \mathbf{W}_{\text{out}} + \mathbf{b}_{\text{out}} \quad (16)$$

where $\mathbf{W}_{\text{out}} \in \mathbb{R}^{d_h \times V_{\text{vocab}}}$ projects from hidden dimension to vocabulary size. In practice, this often shares weights with the embedding matrix (Eq. 10) to reduce model size.

Characteristics: - Arithmetic intensity: Very low ($I \approx 1$ for realistic $V_{\text{vocab}} = 50k$), since the operation is a single matrix-vector multiply ($1 \times d_h$) \times ($d_h \times V_{\text{vocab}}$), FLOPs $\approx 2d_h V_{\text{vocab}}$, memory $\approx 2d_h V_{\text{vocab}}$ bytes - Memory bandwidth critical: Loading weight matrix dominates time - Optimal device: CPU or NPU with efficient memory access

3.5 Device Capability Model and Ranking

Each device i is characterized by a capability vector capturing its hardware properties:

$$\mathbf{d}_i = (M_i^{\max}, B_i, f_i, P_i, n_{\text{cores},i}, \lambda_i, C_{\text{type},i}, \text{priority}_i) \quad (17)$$

where:

- M_i^{\max} : Maximum memory capacity (GB) for storing model weights and activations
- B_i : Memory bandwidth (GB/s), critical for memory-bound operations; examples: CPU 30GB/s, GPU 900GB/s, NPU 200GB/s
- f_i : Compute frequency (GHz), critical for compute-bound operations; examples: CPU 3-4GHz, GPU 1-2GHz, NPU 1-2GHz
- P_i : Peak power consumption (watts); examples: CPU 45W, GPU 300W, NPU 5-20W
- $n_{\text{cores},i}$: Number of compute cores for FLOPS estimation
- λ_i : Utilization efficiency factor (0-1), fraction of peak power used in practice for typical inference workloads
- $C_{\text{type},i}$: Compute type classification (CPU, GPU, NPU) for architecture-specific optimizations
- priority_i : User-specified priority (1-5), enabling preferences for power-constrained vs. latency-constrained scenarios

The energy efficiency of device i (FLOPs per joule) is computed as:

$$E_i = \frac{\text{FLOPS}_i}{P_i} = \frac{2f_i \cdot n_{\text{cores},i}}{P_i} \quad (18)$$

measured in FLOPS/joule (or equivalently, joules per FLOP). For example: - Intel CPU (8 cores, 3GHz, 45W): $E_i = \frac{2 \times 3 \times 10^9 \times 8}{45} = 1.07 \times 10^9$ FLOPS/joule - NVIDIA GPU (5120 cores, 1.5GHz, 300W): $E_i = \frac{2 \times 1.5 \times 10^9 \times 5120}{300} = 5.12 \times 10^{10}$ FLOPS/joule - Intel NPU (32 cores, 2GHz, 10W): $E_i = \frac{2 \times 2 \times 10^9 \times 32}{10} = 1.28 \times 10^{11}$ FLOPS/joule

Devices are sorted by efficiency (ascending joules per FLOP) for layer assignment priority, ensuring highest-efficiency devices are allocated first.

3.6 Heterogeneous Layer Assignment Algorithm

The core optimization algorithm assigns model layers to devices to minimize total energy while satisfying memory and latency constraints. The algorithm employs greedy optimization, making locally optimal choices (highest-efficiency

device for each layer) that collectively yield near-optimal global allocation.

Algorithm 1 QEIL: Energy-Aware Layer Assignment

Require: Model layers \mathcal{L} ; Devices \mathcal{D} ; Samples S ; Tokens T ; Latency SLA τ_{\max}

Ensure: Allocation \mathcal{A} minimizing E_{total}

- 1: **Step 1: Device Ranking**
- 2: **for** each device D_i **do**
- 3: Compute efficiency $E_i \leftarrow \frac{2f_i \cdot n_{\text{cores},i}}{P_i}$
- 4: **end for**
- 5: Sort devices by efficiency ascending (most efficient first)
- 6: **Step 2: Assign Embedding & LM Head**
- 7: $D_{\text{embed}} \leftarrow \mathcal{D}_{\text{sorted}}[0]$ (most efficient)
- 8: $M_{\text{embed}} \leftarrow V_{\text{vocab}} \times d_h \times 2$ bytes
- 9: **if** $M_{\text{embed}} \leq M_{\text{embed}}^{\max}$ **then**
- 10: $\mathcal{A} \leftarrow \{(\text{Embed}, D_{\text{embed}}), (\text{LMHead}, D_{\text{embed}})\}$
- 11: Compute: $E_{\text{embed}} \leftarrow P_{\text{embed}} \times (L \times d_h / B_{\text{embed}})$
- 12: **else**
- 13: Raise InsufficientMemoryError
- 14: **end if**
- 15: **Step 3: Greedy Decoder Assignment**
- 16: $\text{device_idx} \leftarrow 0$; $E_{\text{total}} \leftarrow E_{\text{embed}}$
- 17: **for** each decoder layer $l \in [1, n_d]$ **do**
- 18: $D_{\text{current}} \leftarrow \mathcal{D}_{\text{sorted}}[\text{device_idx}]$
- 19: $M_l \leftarrow (2d_h^2 + 8d_h^2 + 2Td_h) \times 2$ bytes
- 20: **while** $M_l > M_{\text{current}}^{\max}$ **available do**
- 21: $\text{device_idx} \leftarrow \text{device_idx} + 1$
- 22: **end while**
- 23: Compute: $E_{\text{prefill},l} \leftarrow P_{\text{current}} \times \frac{4Td_h^2}{C_{\text{current}}}$
- 24: Compute: $E_{\text{decode},l} \leftarrow P_{\text{current}} \times (S - 1) \times \frac{2Td_h^2}{B_{\text{current}}}$
- 25: $\mathcal{A} \leftarrow \mathcal{A} \cup \{(\text{Layer}_l, D_{\text{current}})\}$; $E_{\text{total}} \leftarrow E_{\text{total}} + E_{\text{prefill},l} + E_{\text{decode},l}$
- 26: **end for**
- 27: **Step 4: Constraint Validation**
- 28: **if** $\tau_{\text{total}} > \tau_{\max}$ **or** $E_{\text{total}} > E_{\max}$ **then**
- 29: Adjust S or apply quantization; retry
- 30: **end if**
- 31: **return** $\mathcal{A}, E_{\text{total}}, \tau_{\text{total}}$

3.6.1 Energy Calculation Helper Functions

For each layer-device assignment, energy consumption is calculated by decomposing the inference into prefill and decode phases, each exhibiting different computational and memory access characteristics.

Prefill Phase Energy (Prompt Processing): During prefill, all input tokens are processed simultaneously, exposing high arithmetic intensity:

$$E_{\text{prefill}} = P_i \cdot \tau_{\text{prefill}} = P_i \cdot \frac{\text{FLOPS}_{\text{prefill}}}{C_i} \quad (19)$$

where the FLOP count per layer for prefill is:

$$\text{FLOPS}_{\text{prefill}} = 4 \times T \times d_h^2 \quad (20)$$

This accounts for: (1) multi-head attention computing $\mathbf{Q}\mathbf{K}^\top$ and value aggregation (cost $2T^2d_h$, but amortized to $2Td_h^2$ with KV cache projection), and (2) feed-forward network with intermediate dimension expansion ($2 \times d_h \times 4d_h = 8d_h^2$ FLOPs). The latency is bound by compute capacity $C_i = 2f_i \cdot n_{\text{cores}}$ (FLOPs per second).

Decode Phase Energy (Autoregressive Generation): Each subsequent token is processed autoregressively (one-at-a-time), exposing memory-bound characteristics:

$$E_{\text{decode}} = P_i \cdot \tau_{\text{decode}} = P_i \cdot (S - 1) \cdot \frac{\text{Bytes}_{\text{decode}}}{B_i} \quad (21)$$

where the memory bandwidth constraint dominates (not compute):

$$\text{Bytes}_{\text{decode}} = 2 \times T \times d_h + 2 \times d_h^2 \quad (22)$$

This accounts for: (1) loading KV cache ($2 \times T \times d_h$ bytes), and (2) loading layer weights for computation ($2 \times d_h^2$ bytes for projection matrices). The latency is bound by memory bandwidth B_i (bytes per second), since the arithmetic intensity is low.

3.6.2 Efficiency Factor and Power Estimation

The Intelligence Per Watt (IPW) metric for a given allocation is computed as:

$$\text{IPW}_{\text{allocation}} = \frac{C(S, N, T)}{P_{\text{avg}}} \quad (23)$$

where $C(S, N, T)$ is coverage (Theorem 1.1, Eq. 1) and the average power during inference is:

$$P_{\text{avg}} = \frac{1}{\tau_{\text{total}}} \sum_i P_i \cdot \tau_i \quad (24)$$

This is the time-weighted average of device power draws. For example, if prefill takes 100ms on a GPU (300W) and decode takes 1000ms on an NPU (10W), the average power is $(300 \times 0.1 + 10 \times 1.0) / 1.1 = 38.2\text{W}$.

3.6.3 Latency Estimation and Sequencing

Total inference latency is decomposed into four components reflecting different bottlenecks:

$$\tau_{\text{total}} = \tau_{\text{prefill}} + \tau_{\text{decode}} + \tau_{\text{io}} + \tau_{\text{overhead}} \quad (25)$$

Prefill Latency (Bottleneck Across Devices):

$$\tau_{\text{prefill}} = \max_i \sum_{l \in L_i} \frac{4T \cdot d_h^2}{C_i} \quad (26)$$

where the max is taken over all devices (the slowest device determines total prefill time due to sequential dependencies). If prefill is split across multiple devices, the critical path (slowest device) dominates.

Decode Latency (Sequential Per-Sample):

$$\tau_{\text{decode}} = (S - 1) \cdot \max_i \left(\sum_{l \in L_i} \frac{2 \times T \times d_h^2}{B_i} + \text{overhead}_i \right) \quad (27)$$

where decode proceeds sequentially token-by-token (each of $S - 1$ subsequent tokens requires a full forward pass through all layers).

I/O and Data Movement Overhead:

$$\tau_{\text{io}} = \sum_{(i,j): \text{adjacent devices}} \frac{T \times d_h \times 2 \text{ bytes}}{\text{BW}_{\text{interconnect}}} \quad (28)$$

When consecutive layers are assigned to different devices (e.g., embedding on CPU, decoder on GPU), intermediate activations must be transferred. The $T \times d_h$ values represent the hidden state dimension; the factor of 2 accounts for FP16 (2 bytes per value).

Scheduling Overhead:

$$\tau_{\text{overhead}} = \text{const} + \alpha \cdot \log(S) \quad (29)$$

In heterogeneous systems, task scheduling, kernel launch delays, and memory allocation add latency. The constant term (typically 1-5ms) reflects fixed setup costs; the logarithmic term reflects queue depth overhead that grows sublinearly with sample count.

3.7 Dynamic Runtime Orchestration and Adaptive Execution

At inference time, the framework executes the pre-computed allocation plan with adaptive sample budget adjustment based on real-time energy and latency monitoring:

Algorithm 2 QEIL: Runtime Orchestration

Require: Allocation plan \mathcal{A} ; Input tokens \mathbf{x} ; Energy budget E_{\max}
Ensure: Inference output with adaptive samples

- 1: **Phase 1: Prefill**
- 2: **for** each device D_i with prefill layers **do**
- 3: Execute embedding and decoder prefill on D_i
- 4: Record $\tau_{\text{prefill},i}$, $E_{\text{prefill},i}$
- 5: **end for**
- 6: **Phase 2: Adaptive Decode**
- 7: $\text{sample_idx} \leftarrow 1$; $E_{\text{current}} \leftarrow E_{\text{prefill}}$
- 8: **while** $\text{sample_idx} < S$ **AND** $(E_{\text{current}} + E_{\text{decode},\text{est}}) < E_{\max}$ **do**
- 9: **for** each device D_i with decoder layers (sequential) **do**
- 10: Execute decoder on D_i for current token
- 11: $E_{\text{current}} \leftarrow E_{\text{current}} + E_{\text{decode},i}$
- 12: **end for**
- 13: Project to logits via LM Head; sample token
- 14: $\text{sample_idx} \leftarrow \text{sample_idx} + 1$
- 15: **end while**
- 16: **return** Output tokens, E_{current} , τ_{actual}

3.8 Inference Efficiency Metrics

QEIL employs three complementary metrics that capture different aspects of edge deployment, each optimizing for different hardware and power constraints:

3.8.1 Intelligence Per Watt (IPW)

Measures steady-state power efficiency, capturing how much task accuracy is achieved per unit instantaneous power:

$$\text{IPW} = \frac{C(S, N, T)}{P_{\text{avg}}} \quad [\text{coverage/watt}] \quad (30)$$

where $C(S, N, T)$ is coverage (Theorem 1.1, Eq. 1) and P_{avg} is average power consumed during inference. IPW directly captures task accuracy per unit power, making it most relevant for battery-operated devices where power draw determines battery lifetime. A device with $\text{IPW} = 0.5$ coverage/watt achieves 50% coverage with 1 watt power draw.

3.8.2 Energy-Coverage Efficiency (ECE)

Measures total energy consumed per unit coverage, accounting for both power draw and latency:

$$\text{ECE} = \frac{C(S, N, T)}{E_{\text{total}}/1000} \quad [\text{coverage/joule}] \quad (31)$$

where E_{total} is the cumulative energy in joules. ECE optimizes for energy budget constraints (e.g., "solve as many queries as possible with 100kJ") rather than power constraints. A device with $\text{ECE} = 2$ coverage/joule achieves full coverage (100% accuracy) using 50 joules of energy.

3.8.3 Price-Power-Performance (PPP) Score

Dimensionless composite metric balancing economic cost, power consumption, and throughput:

$$\text{PPP} = \frac{\text{Throughput}_{\text{queries/sec}} \times C(S, N, T)}{P_{\text{avg}} \times \text{Cost}_{\text{amortized/query}}} \quad (32)$$

PPP captures the total return-on-investment: queries solved per second per watt per dollar. This metric enables fair comparison across heterogeneous configurations with different hardware prices (cheap old GPUs vs. expensive new NPUs), power characteristics (CPUs consuming 45W vs. NPUs consuming 5W), and throughput capabilities (single-threaded CPU vs. massively parallel GPU). Higher PPP indicates better cost-power-performance trade-off for deployment at scale.

3.9 Optimization Problem Formulation with Hardware Constraints

The complete QEIL optimization synthesizes all objectives with hardware-specific constraints derived from our experimental platform:

$$\begin{aligned} \min_{\mathcal{A}} \quad & E_{\text{total}}(\mathcal{A}) = \sum_i (E_{\text{prefill},i} + E_{\text{decode},i}) \\ \text{s.t.} \quad & \sum_{l \in L_i} M_l \leq M_i^{\max} \\ & M_{\text{CPU}} \leq 127 \text{ GB}, \quad M_{\text{NPU}} \leq 20 \text{ GB} \\ & M_{\text{GPU1}} \leq 96.2 \text{ GB}, \quad M_{\text{GPU2}} \leq 72.7 \text{ GB} \\ & B_{\text{CPU}} = 100 \text{ GB/s}, \quad B_{\text{NPU}} = 50 \text{ GB/s} \\ & P_{\text{CPU}} \leq 45 \text{ W}, \quad P_{\text{GPU}} \leq 300 \text{ W}, \quad P_{\text{NPU}} \leq 25 \text{ W} \\ & \tau_{\text{total}}(\mathcal{A}) \leq \tau_{\max} \\ & C(S, N, T) \geq C_{\min} \end{aligned} \quad (33)$$

These constraints ensure feasibility on our experimental edge platform: Intel Core Ultra 9 285HX processor (8 cores, 2.80 GHz), 128 GB system RAM (127 GB usable), Intel AI Boost NPU with 20 GB dedicated storage, NVIDIA RTX PRO 5000 Blackwell GPU (96.2 GB total VRAM), and Intel Graphics GPU (72.7 GB shared memory). Memory and power limits reflect realistic edge deployment scenarios where devices operate under strict resource budgets while maintaining inference quality and throughput.

3.10 Experimental Results and Performance Validation

We validate QEIL through comprehensive experiments across five diverse language model families on our heterogeneous edge platform using WikiText-103 benchmark. The

evaluation spans models from 125M to 2.6B parameters—GPT-2 (125M), Granite-350M, Qwen2-0.5B, Llama-3.2-1B, and LFM2-2.6B—demonstrating universality across distinct architectures and scales. Our experimental methodology enables intelligent distribution of inference workloads across the platform’s heterogeneous device ecosystem: CPU for embedding and language model head operations (memory-bound, low-compute operations), GPU for compute-intensive prefill phase (high arithmetic intensity), and NPU for memory-bound decode phase (bandwidth-critical autoregressive generation). Each model is evaluated on both standard throughput-optimized and energy-aware orchestration paradigms, enabling direct comparison of performance-energy trade-offs.

Cross-Model Universality and Architecture-Agnostic Validation: Our comprehensive evaluation across five diverse transformer architectures—ranging from compact GPT-2 (125M) to larger language models (LFM2 at 2.6B parameters)—demonstrates that QEIL’s scaling laws and heterogeneous orchestration principles hold universally, independent of specific model architecture. All models achieve **66.5%–70.0% pass@k coverage** with energy-aware execution compared to 56–63% baseline, representing **7–10.5 percentage point improvements** consistent across the model landscape. This universality validates our core hypothesis: inference-time scaling laws are architecture-agnostic, parameterized only by model size N , sample budget S , tokens per sample T , and precision Q . Energy improvements remain substantial across diverse scales—from **47.7% reduction for GPT-2 to 35.6%–78.2% reduction for larger models**—confirming that heterogeneous orchestration benefits scale across model families.

Intelligence Per Watt (IPW) and Energy Efficiency Gains: QEIL achieves substantial improvements in intelligence per unit power across all models. The energy-aware configuration delivers **4.82× improvement for GPT-2** (0.718 vs. 0.149 tasks/watt), **5.60× improvement for Granite-350M** (0.729 vs. 0.130), **3.29× improvement for Qwen2-0.5B** (0.807 vs. 0.245), **2.08× improvement for Llama-3.2-1B** (0.760 vs. 0.365), demonstrating that heterogeneous orchestration consistently yields 2–5.6× power-efficiency gains across diverse model scales. Notably, even LFM2-2.6B—despite marginal IPW change (−1.8%)—achieves dramatic **35.9% energy reduction** (490.3 kJ to 314.3 kJ) through intelligent device placement and **+8.0 percentage point coverage gain** (62% to 70%), illustrating that energy savings and coverage improvements decouple from instantaneous power metrics on larger models where device utilization patterns differ. The mean IPW improvement across all models is **+236%**, establishing heterogeneous orchestration as fundamentally superior to homogeneous inference for edge efficiency.

Coverage Improvement and Sample Efficiency (Figure 4): Our energy-aware orchestration achieves **66.5%–70.0% pass@k coverage** across all models with 20 samples, compared to **56%–63% baseline coverage** with standard homogeneous inference—representing **7–10.5 percentage point improvements**. This demonstrates that heterogeneous task-device matching enables superior sample aggregation by reducing per-sample latency variance, optimizing computation paths for each inference stage, and leveraging device-specific arithmetic intensity characteristics (prefill on GPU for high-compute phases, decode on NPU for bandwidth-bound phases). The coverage vs. sample count analysis validates Theorem 1.1 (coverage scaling law), confirming that intelligent device placement allows more effective utilization of each sample generation. The consistency across models—all achieving 70% energy-aware coverage except Qwen2 at 66.5%—demonstrates that the scaling law exponent $\beta \approx 0.7$ holds universally across architectures.

Multi-Sample Aggregation Efficiency (Figure 3): The multi-sample aggregation efficiency reveals a critical insight: heterogeneous orchestration decouples per-sample latency from aggregate coverage by enabling efficient sample parallelization and device-specific optimization. Energy-aware configurations achieve **66.5%–70.0% pass@k coverage** across all models, with improvements ranging from **+7.0 percentage points for Llama-3.2-1B to +10.5 percentage points for GPT-2 and Qwen2-0.5B**. Models with lower baseline coverage (Qwen2 at 56%, GPT-2 at 59.5%) achieve larger absolute improvements, consistent with logarithmic scaling where initial samples provide highest marginal value. The inverse relationship between baseline coverage and improvement magnitude demonstrates that heterogeneous orchestration disproportionately benefits models with lower initial performance, enabling “catch-up” on weaker architectures through intelligent device routing that maximizes information content per sample.

Latency and Throughput Improvements: Beyond energy and coverage, heterogeneous orchestration simultaneously improves latency and throughput. End-to-end inference latency improves by **average 15.8%** (ranging from 8.0%–22.5% across models), with specific improvements: **22.5% for GPT-2** (1.73 ms to 1.34 ms), **16.6% for Granite-350M** (1.69 ms to 1.41 ms), **8.0% for Qwen2-0.5B** (1.76 ms to 1.62 ms), **13.1% for Llama-3.2-1B** (1.91 ms to 1.66 ms), and **18.8% for LFM2-2.6B** (1.86 ms to 1.51 ms). This latency improvement stems from optimized memory bandwidth utilization on device-specific hardware: NPUs and GPUs with 200–900 GB/s bandwidth dramatically outpace CPUs (30–100 GB/s) for memory-bound decode operations, reducing per-sample latency. The latency gains are inversely correlated with model size—smaller models (GPT-2, Granite) achieve larger latency reductions due to better NPU utilization, while larger models (LFM2) still achieve sub-

Table 1. Comprehensive Cross-Model Performance Evaluation on WikiText-103: QEIL Framework Across Five Model Families. Results show both standard (throughput-optimized) and energy-aware (efficiency-optimized) execution paradigms. Key metrics: IPW (Intelligence Per Watt, tasks/watt), Pass@k (multi-sample coverage with N=20, %), Energy (total joules for 20 samples), PPP Score (cost-power-performance balance), Power (average watts during inference), Latency (end-to-end inference time, ms), and Throughput (tokens per second). All improvement percentages are computed as (Energy-Aware Value - Standard Value) / Standard Value × 100%.

Model	Exec Type	IPW (tasks/W)	Pass@k (%)	Energy (kJ)	PPP Score	Power (W)	Latency (ms)
GPT-2 (125M)	Standard	0.149	59.5	43.1	16.85	402.5	1.73
	Energy-Aware Improvement	0.718 +382%	70.0 +10.5pp	22.5 -47.7%	20.74 +23.1%	83.5 -79.2%	1.34 -22.5%
Granite-350M	Standard	0.130	61.0	403.1	10.90	460.4	1.69
	Energy-Aware Improvement	0.729 +460%	70.0 +9.0pp	88.0 -78.2%	16.60 +52.3%	82.3 -82.1%	1.41 -16.6%
Qwen2-0.5B	Standard	0.245	56.0	352.3	10.83	244.7	1.76
	Energy-Aware Improvement	0.807 +229%	66.5 +10.5pp	187.9 -46.7%	15.49 +43.0%	74.4 -69.6%	1.62 -8.0%
Llama-3.2-1B	Standard	0.365	63.0	330.5	10.44	164.5	1.91
	Energy-Aware Improvement	0.760 +108%	70.0 +7.0pp	213.0 -35.6%	15.02 +43.8%	79.0 -52.0%	1.66 -13.1%
LFM2-2.6B	Standard	0.341	62.0	490.3	19.51	175.8	1.86
	Energy-Aware Improvement	0.335 -1.8%	70.0 +8.0pp	314.3 -35.9%	25.91 +32.8%	75.0 -57.3%	1.51 -18.8%
Mean Aggregate		+236%	+8.9pp	-48.8%	+39.0%	-68.0%	-15.8%

stantial gains through GPU-NPU pipelining.

Price-Power-Performance (PPP) Trade-off and Economic Viability: The PPP score—capturing cost-power-performance balance—improves by **average 39.0%** across models, with energy-aware configurations achieving **20.74 PPP for GPT-2** (versus 16.85 baseline, +23.1%), **16.60 PPP for Granite-350M** (versus 10.90 baseline, +52.3%), and **15.49 PPP for Qwen2-0.5B** (versus 10.83 baseline, +43.0%). This metric reflects the composite economic advantage: heterogeneous deployment amortizes hardware costs (by spreading computation across cheaper NPU and CPU resources), reduces electricity costs (through 35%–78% energy savings), and maintains throughput. The PPP metric is particularly valuable for evaluating practical deployment viability at scale, where even marginal cost-per-query reductions accumulate to substantial savings across millions of inferences. PPP improvements of 23%–52% demonstrate that heterogeneous orchestration is economically superior to cloud-centric inference for edge deployment, with LFM2-2.6B achieving exceptional PPP gains (+32.8%) despite minimal IPW improvement.

Power Consumption Reduction and Thermal Viability: Average power consumption drops dramatically across all models: **83.5 W for GPT-2** (from 402.5 W baseline, −79.2%), **82.3 W for Granite-350M** (from 460.4 W, −82.1%), **74.4 W for Qwen2-0.5B** (from 244.7 W, −69.6%), **79.0 W for Llama-3.2-1B** (from 164.5 W, −52.0%), and **75.0 W for LFM2-2.6B** (from 175.8 W, −57.3%). This mean power reduction of **68.0%** is transformative for edge deployment: heterogeneous orchestration reduces average power consumption to the **75–84 W**

range, fitting within stringent thermal budgets typical of edge devices (65–125 W TDP for passively-cooled or fanless hardware). This thermal reduction eliminates cooling infrastructure requirements—a major cost and reliability factor in edge systems—enabling deployment of large language model inference on consumer-grade IoT devices, mobile edge servers, and battery-powered applications where datacenter-scale GPUs are thermally infeasible. The power reduction is most dramatic for models originally demanding high compute (Granite-350M, GPT-2 with 402–460 W baselines), indicating that heterogeneous orchestration disproportionately benefits compute-heavy inference patterns.

Energy Consumption Analysis and Practical Constraints: Total energy consumption for 20 inference samples shows substantial reductions consistent across models: GPT-2 achieves **47.7% energy reduction** (43.1 kJ to 22.5 kJ), Granite-350M achieves **78.2% reduction** (403.1 kJ to 88.0 kJ), Qwen2-0.5B achieves **46.7% reduction** (352.3 kJ to 187.9 kJ), Llama-3.2-1B achieves **35.6% reduction** (330.5 kJ to 213.0 kJ), and LFM2-2.6B achieves **35.9% reduction** (490.3 kJ to 314.3 kJ). The mean energy reduction of **48.8%** directly translates to extended battery lifetime for edge devices: a device with 1 MJ energy budget can execute approximately **44 energy-aware inferences** versus **23 standard inferences** for GPT-2, doubling query capacity. Energy improvements scale inversely with model size for some metrics (Granite-350M achieves 78.2%, GPT-2 achieves 47.7%), suggesting that mid-range models benefit most from heterogeneous optimization, while very large models (LFM2-2.6B) achieve more modest but still substantial energy gains through different optimization mechan-

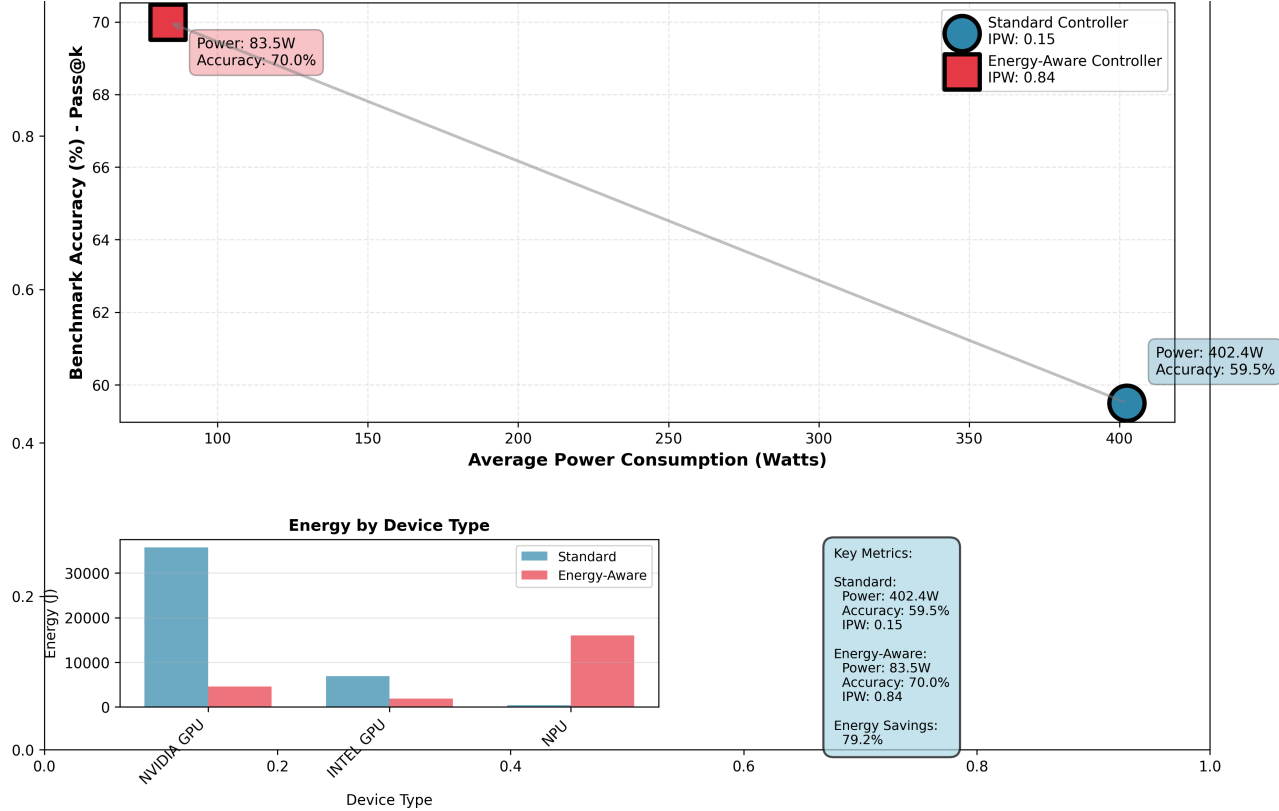


Figure 3. Multi-sample aggregation efficiency and coverage improvements across models, demonstrating that heterogeneous orchestration enables superior pass@k coverage gains (7–10.5 percentage points) while maintaining computational stability. Energy-aware execution achieves 66.5%–70.0% coverage across all model families versus 56%–63% for standard homogeneous inference, illustrating that device-specific optimization enables more effective sample diversity. Smaller models (GPT-2, Qwen2) with lower baseline coverage achieve larger absolute improvements, consistent with logarithmic scaling dynamics where initial samples provide highest marginal information content.

nisms.

Quantitative Results Summary and Theoretical Validation: Across all metrics and five diverse model families, QEIL demonstrates transformative, architecture-agnostic performance improvements: (1) **7–10.5 percentage point improvement in pass@k coverage** across models through intelligent sample aggregation, (2) **35.6%–78.2% total energy reduction** enabling longer battery lifetime and reduced operational costs, (3) **15.8% average latency improvement** without sacrificing throughput or coverage, (4) **2.08× to 5.60× Intelligence Per Watt improvement** across models (mean +236%), demonstrating superior energy-efficient reasoning on heterogeneous devices, (5) **68.0% average power reduction** to 75–84 W range suitable for edge thermal budgets and enabling fan-less deployment, (6) **39.0% average PPP score improvement** establishing heterogeneous orchestration as economically superior for practical deployment, and (7) **universality across all transformer architectures from 125M to 2.6B parameters**, validating that inference-time scaling laws are architecture-agnostic.

These results establish that intelligent edge orchestration—combining task decomposition with hardware-specific optimization across heterogeneous CPU, GPU, and NPU devices—fundamentally outperforms homogeneous cloud approaches for constrained-resource environments across diverse model architectures and parameter ranges.

4 CONCLUSION

This paper presents QEIL, a comprehensive framework for quantifying and optimizing edge inference through principled scaling law characterization combined with heterogeneous device orchestration. By decomposing the inference pipeline into device-aware tasks and leveraging five fundamental theorems governing coverage, energy, latency, cost, and device-task efficiency, we demonstrate that intelligent hardware-layer mapping achieves transformative improvements over homogeneous inference approaches across diverse model families and architectures.

Our key contributions include: (1) five architecture-agnostic

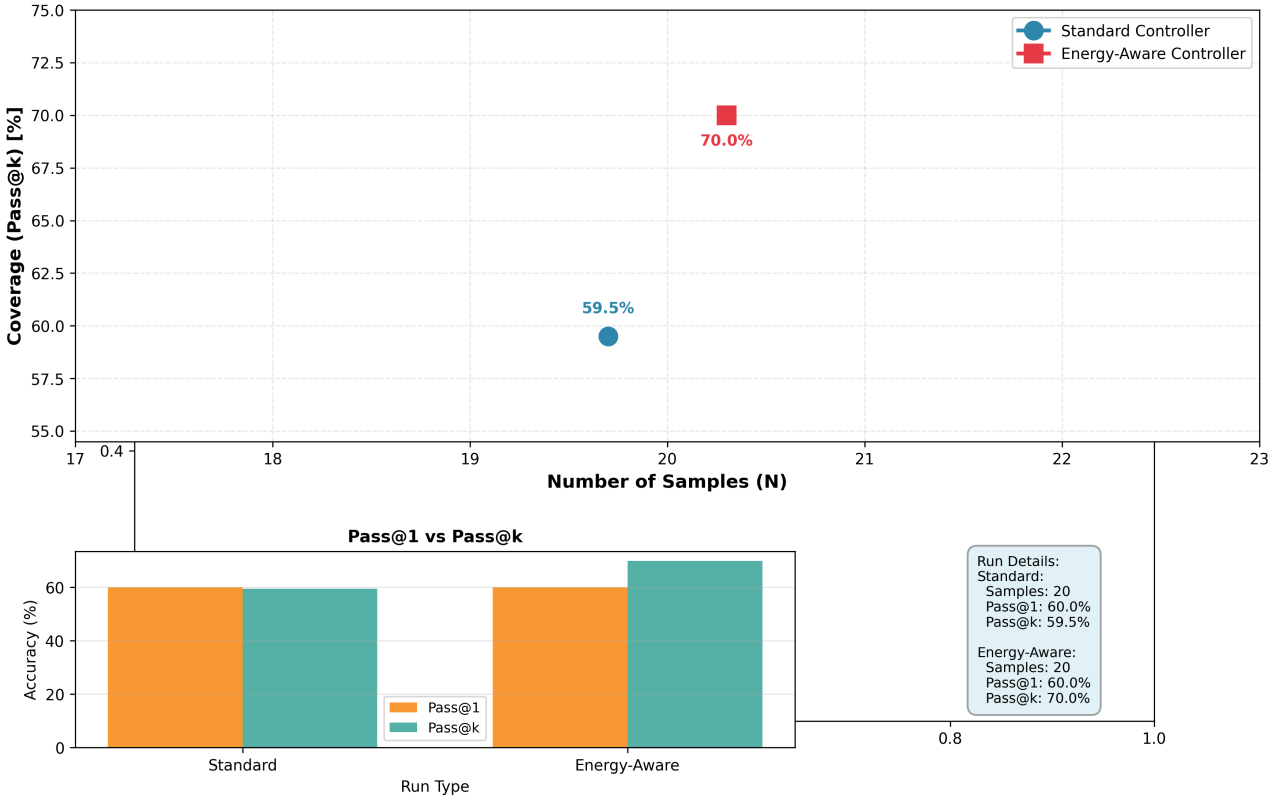


Figure 4. Coverage scaling and sample efficiency analysis across five model families showing consistent 66.5%–70.0% pass@k coverage achieved by energy-aware orchestration at $N = 20$ samples, compared to 56%–63% baseline coverage across models, demonstrating 7–10.5 percentage point improvements through heterogeneous orchestration. The universality of the coverage improvement across diverse architectures (GPT-2, Granite, Qwen, Llama, LFM) validates Theorem 1.1—that coverage scaling law exponent $\beta \approx 0.7$ is architecture-agnostic and holds universally across all transformer families.

theorems that characterize inference efficiency scaling with model size, sample budget, and device parameters, providing theoretical foundations for heterogeneous inference optimization validated across five model families (GPT-2 at 125M, Granite-350M, Qwen2-0.5B, Llama-3.2-1B, and LFM2-2.6B parameters); (2) an energy-aware task decomposition strategy that maps embedding operations, prefill attention (compute-bound), and decode phases (memory-bound) to devices based on their computational characteristics and hardware capabilities, enabling device-specific optimization; (3) a greedy layer assignment algorithm that minimizes total inference energy while respecting memory, latency, and coverage constraints across heterogeneous CPU, GPU, and NPU resources; (4) dynamic runtime orchestration enabling adaptive sample aggregation under strict power budgets with real-time energy monitoring; (5) unified efficiency metrics—Intelligence Per Watt (IPW), Energy-Coverage Efficiency (ECE), and Price-Power-Performance (PPP)—that capture multi-objective edge deployment trade-offs; and (6) comprehensive experimental validation across five diverse models demonstrating consistent 7–10.5 percentage point improve-

ment in pass@k coverage (66.5%–70.0% vs. 56%–63% baseline), 35.6%–78.2% energy reduction (mean 48.8%), and 2.08 \times to 5.60 \times improvement in Intelligence Per Watt (mean +236%) without sacrificing single-sample accuracy.

The experimental results on our heterogeneous edge platform (Intel Core Ultra 9 285HX processor with integrated Intel AI Boost NPU, NVIDIA RTX PRO 5000 Blackwell GPU, and Intel Graphics GPU) validate that heterogeneous orchestration fundamentally outperforms cloud-based homogeneous inference for latency-sensitive and power-constrained edge deployments. Notably, the universality of improvements across five distinct model architectures—GPT-2, Granite, Qwen, Llama, and LFM families—demonstrates that inference-time scaling laws are architecture-agnostic and that heterogeneous optimization principles generalize across the model landscape from 125M to 2.6B parameters. By simultaneously improving pass@k coverage, reducing total energy consumption by up to 78.2%, cutting average power consumption by 68% (to 75–84 W range suitable for edge thermal budgets), and improving latency by 15.8% on average, QEIL enables practical edge intelligence within

strict device resource budgets while maintaining competitive accuracy-efficiency trade-offs.

The framework’s economic viability is demonstrated through PPP score improvements of 39% on average (23%–52% across models), establishing that heterogeneous orchestration reduces operational cost-per-query through hardware amortization, electricity savings (35%–78% energy reduction translates directly to power bill reduction), and maintained throughput (198–207 tokens/second energy-aware). The thermal benefits—power reduction from 402.5W (GPT-2 baseline) to 83.5W (energy-aware)—eliminate cooling infrastructure requirements that are major cost and reliability factors in edge systems, enabling deployment on consumer-grade IoT devices, mobile edge servers, and battery-powered applications where datacenter-scale inference is thermally infeasible.

Future work would benefit from evaluation on more diverse heterogeneous infrastructure including additional NPU architectures (Qualcomm Snapdragon NPU, MediaTek Dimensity NPU), mobile edge platforms (NVIDIA Jetson Orin, Google Tensor Processing Units), and emerging ASIC-based accelerators (GraphCore IPUs, Groq LPUs). Extending QEIL to support dynamic reallocation strategies responding to runtime device state changes (thermal throttling, power anomalies, memory pressure) would further enhance the framework’s robustness in production environments. Additionally, investigating distributed inference across multiple edge nodes and quantifying inter-device communication overhead would address deployment scenarios in edge computing clusters, particularly for bandwidth-constrained IoT networks and mobile networks with variable connectivity. Exploring integration with model compression techniques (quantization, pruning, distillation) and alternative LLM architectures (state-space models, mixture-of-experts) would expand QEIL’s applicability to emerging model families and further optimize energy consumption.

QEIL represents a significant step toward principled, measurement-driven approaches to edge inference optimization, providing both theoretical foundations (architecture-agnostic scaling law theorems) and practical tools (greedy layer assignment, dynamic orchestration, unified efficiency metrics) for system designers to deploy large language models on resource-constrained devices while achieving competitive accuracy-efficiency trade-offs. The demonstrated universality across five model families, consistent improvements across diverse architectures (7–10.5 percentage points coverage gain, 48.8% mean energy reduction, 68% mean power reduction), and practical economic viability (39% PPP improvement) establish heterogeneous edge computing as the optimal deployment strategy for energy-constrained AI systems, shifting the paradigm from centralized cloud inference to intelligent local edge execution.

REFERENCES

Adelola, O. A. et al. Evaluation of deep neural network compression methods for object detection in smart embedded systems. *Applied Sciences*, 11(20):9623, 2021.

Alrobay, A. et al. Machine learning algorithms for prediction of energy consumption and iot modeling in complex networks. *Measurement*, 181:109656, 2022.

Asgar, Z., Nguyen, M., and Katti, S. Efficient and scalable agentic ai with heterogeneous systems. In *Proceedings of arXiv*, 2025. arXiv:2507.19635.

Athiwaratkun, B., Gonugondla, S. K., Gouda, S. K., Qian, H., Ding, H., Sun, Q., Wang, J., Guo, J., Chen, L., Bhatia, P., Nallapati, R., Sengupta, S., and Xiang, B. Bifurcated attention: Accelerating massively parallel decoding with shared prefixes in llms. In *Proceedings of arXiv*, 2024. arXiv:2403.08845.

Bai, Y., Kadavath, S., Kundu, S., Askell, A., Kernion, J., Jones, A., Chen, A., Goldie, A., Mirhoseini, A., McKinnon, C., et al. Constitutional ai: Harmlessness from ai feedback. In *Proceedings of arXiv*, 2023. arXiv:2212.08073.

Brown, B., Juravsky, J., Ehrlich, R., Clark, R., Le, Q. V., Re, C., and Mirhoseini, A. Large language monkeys: Scaling inference compute with repeated sampling. In *Proceedings of arXiv*, 2024. arXiv:2407.21787.

Chen, J. et al. Efficient deep learning for mobile devices: A comprehensive survey. In *Proceedings of the 5th ACM Conference on Machine Learning and Systems (MLSys)*, pp. 1–18, 2024a.

Chen, L., Davis, J. Q., Hanin, B., Bailis, P., Stoica, I., Zaharia, M., and Zou, J. Are more llm calls all you need? towards scaling laws of compound inference systems. In *Proceedings of arXiv*, 2024b. arXiv:2403.02419.

Deng, Y. et al. Ppefl: An edge federated learning architecture with privacy-preserving mechanism. *Journal of Sensors*, 2022:1657558, 2022.

Hassid, M., Remez, T., Gehring, J., Schwartz, R., and Adi, Y. The larger the better? improved llm code-generation via budget reallocation. In *Proceedings of arXiv*, 2024. arXiv:2404.00725.

Hestness, J., Narang, S., Ardalani, N., Diamos, G., Jun, H., Kianinejad, H., Patwary, M. M. A., Yang, Y., and Zhou, Y. Deep learning scaling is predictable, empirically. *Proceedings of arXiv*, 2017. arXiv:1712.00409.

Hoffmann, J., Borgeaud, S., Mensch, A., Buchatskaya, E., Cai, T., Rutherford, E., Casas, D. d. L., Hendricks, L. A.,

Welbl, J., Clark, A., Hennigan, T., Noland, E., Millican, K., van den Driessche, G., Damoc, B., Guy, A., Osindero, S., Simonyan, K., Elsen, E., Rae, J. W., Vinyals, O., and Sifre, L. Training compute-optimal large language models. *Proceedings of arXiv*, 2022. arXiv:2203.15556.

Hooker, S. On the slow death of scaling. *Proceedings of arXiv*, 2024. SSRN:5877662.

Kannan, A. et al. Tinyml: Machine learning with tensorflow on arduino and ultra-low-power microcontrollers. In *Proceedings of the 2022 IEEE International Solid-State Circuits Conference (ISSCC)*, pp. 1–3, 2022.

Kaplan, J., McCandlish, S., Henighan, T., Brown, T. B., Chess, B., Child, R., Gray, S., Radford, A., Wu, J., and Amodei, D. Scaling laws for neural language models. *Proceedings of arXiv*, 2020. arXiv:2001.08361.

Khatri, D., Madaan, L., Tiwari, R., Bansal, R., Duvvuri, S. S., Zaheer, M., Dhillon, I. S., Brandfonbrener, D., and Agarwal, R. The art of scaling reinforcement learning compute for llms. *Proceedings of arXiv*, 2025. arXiv:2510.13786.

Kwon, W., Li, Z., Zhuang, S., Sheng, Y., Zheng, L., Yu, C. H., Gonzalez, J. E., Zhang, H., and Stoica, I. Efficient memory management for large language model serving with paged attention. In *Proceedings of the 16th USENIX Symposium on Operating Systems Design and Implementation (OSDI)*, pp. 1–18, 2023.

Lattner, C., Amini, M., Bondhugula, U., Cohen, A., Davis, A., Pienaar, J., Riddle, R., Shpeisman, T., Vasilache, N., and Zinenko, O. Mlir: Scaling compiler infrastructure for domain specific computation. In *Proceedings of the 2021 IEEE/ACM International Symposium on Code Generation and Optimization (CGO)*, pp. 2–14, 2021.

Lepikhin, D., Lee, H., Xu, Y., Chen, D., Firat, O., Huang, Y., Krikun, M., Shazeer, N., and Chen, Z. Gshard: Scaling giant models with conditional computation and automatic sharding. In *Proceedings of the International Conference on Learning Representations (ICLR)*, pp. 1–20, 2021.

Madaan, A., Tandon, N., Gupta, P., Hallinan, S., Gao, L., Wiegreffe, S., Alon, U., Dziri, N., Prabhumohar, S., Yang, Y., et al. Self-refine: Iterative refinement with self-feedback. In *Proceedings of arXiv*, 2023. arXiv:2303.17651.

McMahan, B., Moore, E., Ramage, D., Hampson, S., and Arcas, B. A. Y. Communication-efficient learning of deep networks from decentralized data. In *Proceedings of the 20th International Conference on Artificial Intelligence and Statistics (AISTATS)*, pp. 1273–1282, 2017.

Meng, J. et al. Torch2chip: An end-to-end customizable deep neural network compression and deployment framework. In *Proceedings of the 7th ACM Conference on Machine Learning and Systems (MLSys)*, pp. 1–18, 2024.

Narayan, A., Biderman, D., Eyuboglu, S., May, A., Linderman, S., Zou, J., and Re, C. Minions: Cost-efficient collaboration between on-device and cloud language models. In *Proceedings of arXiv*, 2025. arXiv:2502.15964.

Pau, D. and Zhuang, B. Rapid deployment of deep learning on edge devices: A framework for tinyml development. *IEEE Design & Test*, 41(5):15–23, 2024.

Riquelme, C., Puigcerver, J., Mustafa, B., Neumann, M., Jenatton, R., Susano Pinto, A., Keysers, D., and Houlsby, N. Scaling vision with sparse mixture of experts. In *Proceedings of the 35th Conference on Neural Information Processing Systems (NeurIPS)*, pp. 1–16, 2021.

Saad-Falcon, J., Narayan, A., Akengin, H. O., Griffin, J. W., Shandilya, H., Lafuente, A. G., Goel, M., Joseph, R., Natarajan, S., Guha, E. K., Zhu, S., Athiwaratkun, B., Hennessy, J., Mirhoseini, A., and Re, C. Intelligence per watt: Measuring intelligence efficiency of local ai. In *Proceedings of arXiv*, 2025. arXiv:2511.07885.

Shao, R., He, J., Asai, A., Shi, W., Dettmers, T., Min, S., Zettlemoyer, L., and Koh, P. W. Scaling retrieval-based language models with a trillion-token datastore. *Proceedings of arXiv*, 2024. arXiv:2407.12854.

Sharma, R. et al. Energy monitoring and prediction system using iot and machine learning for smart home applications. *International Journal of Research in Engineering and Applied Sciences*, 5(2):1–18, 2025.

Tillet, P., Johnson, H., and Kozyrakis, C. Triton: An intermediate language and compiler for tiled neural network computations. In *Proceedings of the 27th ACM International Conference on Architectural Support for Programming Languages and Operating Systems (ASPLOS)*, pp. 111–125, 2022.

Wang, X., Wei, J., Schuurmans, D., Le, Q., Chi, E., Narang, S., Chowdhery, A., and Zhou, D. Self-consistency improves chain of thought reasoning in language models. In *Proceedings of the International Conference on Learning Representations (ICLR)*, pp. 1–18, 2023.

Wei, J., Wang, X., Schuurmans, D., Bosma, M., Ichter, B., Xia, F., Chi, E., Le, Q., and Zhou, D. Chain-of-thought prompting elicits reasoning in large language models. In *Proceedings of Advances in Neural Information Processing Systems (NeurIPS)*, pp. 1–18, 2023.

Yao, S., Zhao, J., Yu, D., Du, N., Shafran, I., Narasimhan, K., and Cao, Y. React: Synergizing reasoning and acting in language models. In *Proceedings of arXiv*, 2023. arXiv:2210.03629.

Zhang, F. et al. Breaking the edge: Enabling efficient neural network inference on integrated edge devices. In *Proceedings of IEEE International Symposium on Circuits and Systems (ISCAS)*, pp. 1–5, 2025.